Expression strategies for structural studies of eukaryotic membrane proteins

Joseph A. Lyons[1,2,3*], Azadeh Shahsavar[1,2,3,4*], Peter Aasted Paulsen[3], Bjørn Panyella Pedersen[3], Poul Nissen[1,2,3]

* these authors contributed equally

Affiliations
1] Danish Research Institute of Translational Neuroscience (DANDRITE), Nordic EMBL Partnership for Molecular Medicine, Aarhus University, Aarhus, Denmark.
[2] Centre for Membrane Pumps in Cells and Disease - PUMPkin, Danish National Research Foundation, Aarhus, Denmark
[3] Department of Molecular Biology and Genetics, Aarhus University, Aarhus, Denmark.
[4] EMBL, Notkestrasse 85, 22607 Hamburg, Germany

Abstract

Integral membrane proteins in eukaryotes are central to various cellular processes and key targets in structural biology, biotechnology and drug development. However, the number of available structures for eukaryotic membrane protein belies their physiological importance. Recently, the number of available eukaryotic membrane protein structures has been steadily increasing due to the development of novel strategies in construct design, expression and structure determination. Here, we examine the major expression systems exploited for eukaryotic membrane proteins. Additionally we strive to tabulate and describe the recent expression strategies in eukaryotic membrane protein structural biology. We find that a majority of targets have been expressed in advanced host systems and modified from their wild-type form with distinct focus on conformation and thermo-stabilisation. However, strategies for native protein purification should also be considered where possible, particularily in light of the recent advances in single particle cryo electron microscopy.

Introduction

Integral membrane proteins (IMPs) undertake a myriad of cellular functions, which range from sensory stimuli transduction and catalysis to transport and energy transduction. IMPs account for approximately 30% of all protein-coding genes in humans and are important targets for pharmaceuticals and drug development. The structures obtained to date reflect only a tiny fraction and generally represent the most tractable targets, i.e., those expressed to high abundance either natively or through recombinant systems. However, the rate by which new structures of IMPs and in particular eukaryotic integral membrane proteins (eIMP) emerge is steadily increasing due in no small part to innovative protein expression, engineering and structure determination strategies developed over the last few years [1].

In this review, we compare and contrast the various expression systems available for eIMPs with a focus on the last two years (Supplementary Table 1). We extract recent advances and summarise the general principles emerging in the field of eIMP structural biology.

Expressions systems

Early structures of eukaryotic membrane proteins exploited the natural abundance of selected targets. Native sources remain a significant source of structural information (Supplementary Table 1, Figure 1a), and likely will remain so also in the future with the recent rise of single particle cryo-electron microscopy (cryo-EM) as typified by the structures of the inositol-1,4,5-trisphosphate (IP3) receptor[2], the ryanodine receptor[3, 4] and the voltage-gated calcium channel Cav1.1 complex[5]. For the latter two, the respective native proteins were purified by a pull-down purification approach using a recombinant GST-fused accessory protein[4, 5]. CRISPR technology may also be helpful to introduce affinity tags or proteolytic sites into target proteins in a native background.

The majority of eIMPs however are expressed at very low levels in native sources, so recombinant over-expression is required for structural and functional characterisation. The choice of an expression system for an eIMP target is generally

dictated by 1) the locally accessible expression systems, where already present knowledge and experience can significantly improve productivity, 2) the nature and complexity of the chosen target, and 3) cost. Typically, the expression of a range of homologs representing a variety of species are screened for the best and most stable expressing proteins, although for drug development a close homology to the pharmacological target will be required. Indeed, for bacterial to mammalian expression systems, high-throughput pipelines exist for the evaluation of GFP fusion constructs based on expression and sample homogeneity using fluorescence size exclusion chromatography as reviewed elsewhere [6-11].

Bacteria

The most common bacterial expression system, *Escherichia coli* (*E. coli*) is a rapid, versatile and cost effective expression system. The system has limitations due to different protein folding chaperones and a lack of essential lipids and post-translational modifications (PTMs) required for proper eIMP expression. Despite the many attempts to improve the expression of active eIMPs in *E. coli* including co-expression of molecular chaperones, tagging the target protein with a fusion protein and co-expression of post-translational machineries[12], *E. coli* remains a challenged system for the over-expression of eIMPs (Supplementary Table 1, Figure 1). Indeed, of the 11 eIMP structures derived from *E. coli* expression (Supplementary Table 1), over half were either fragments or required refolding.

Yeasts

Yeast was the first successful system for recombinant expression of eIMPs for crystallographic studies[13, 14]. The most common yeast strains for the over-expression of eIMPs for structural studies are *Saccharomyces cerevisiae* (*S. cerevisiae*)[7, 8, 14] and the methylotrophic *Pichia Pastoris* (*P. pastoris*) [6, 15-17] (Supplementary Table 1). Both strains are cost effective eukaryotic expression systems capable of performing various PTMs including high mannose *N*-glycosylation. However, the absence of specific sterols might be one of the reasons that only a limited number of eIMP structures have been obtained using yeast expression systems (Figure 1b and c, Supplementary Table 1).

Expression in *P. pastoris* uses an integrated vector compared to the multicopy plasmid system in *S. cerevisiae*. The most common vector used in *P. pastoris* expression system, pPICZ, uses a promoter derived from the alcohol oxidase I (AOXI) gene, which is inducible by methanol and carries a simple drug-based selection system (Zeocin). Most vectors used in *S. cerevisiae* expression systems are propagated using the high copy 2-micron plasmid replication origin[18]. Recently, taking advantage of incorporating a defective *leu2-d* gene, in addition to the primary selection marker, has promoted an even higher plasmid copy number under leucine deficient growth conditions leading to improved expression levels[19-21]. Expression in *S. cerevisiae* mostly utilizes GAL1, a strong inducible promoter, which drives expression of the target gene following depletion of glucose and addition of galactose as the carbon source during culturing.

Insect cell

Baculovirus transduction of insect cells is the dominant heterologous expression system for the production of eIMPs, especially mammalian/human targets that have yielded structures over the past two years including a surge of G-protein coupled receptors (Figure 1). The gene of interest is cloned into the pFastBac vector, which controls the expression of the target gene by either the strong *Autographa californica* multiple nuclear polyhedrosis virus (AcMNPV) polyhedrin (PH) or p10 promoters. The vector is then used to produce a recombinant baculovirus shuttle vector (bacmid) [22] to transfect the insect cells for expression of the target protein [23]. This can be further adapted for the expression of multi-gene complexes using the Multibac system as reviewed in [24-26]. The two most common insect cell lines are *Spodoptera frugiperda* (*sf*9 and *sf*21) and *Trichoplusia ni* (*Hi*5). The majority of eIMPs structures are obtained from the *S. frugiperda* expression system (Figure 1).

Lipid content, PTMs and protein folding in insect cells more closely resemble mammalian than bacterial and yeast systems. However, *N*-glycosylation in insect cells results in simple oligo-mannose sugar chains, while mammalian cells produce more complex *N*- glycans containing terminal sialic acids, which is a limitation as *N*-glycans often contribute to the functionality of the glycoprotein [27]. Engineered insect cell lines that express the enzymes required for mammalian-like glycosylation patterns can produce complex terminally sialylated *N*-glycans if required[28-30].

Mammalian cell

The need for specific PTMs and a near-native-like lipid environment for some mammalian membrane proteins make the use of mammalian cell expression systems highly desirable [1]. The human embryo kidney (HEK) and Chinese hamster ovary (CHO) are the two most common mammalian cell lines for recombinant expression of membrane proteins. While both cell lines can be subjected to transient and stable transfections [31], transient transfection of HEK293SGnTI− (*N*-acetylglucosaminyl-transferase I–negative) is responsible for the majority of eIMPs whose structures are deposited in PDB over the past two years (Supplementary Table 1). Despite the slow growth rate and traditionally higher cost of mammalian expression systems [32], the number of structures generated based on such systems has considerably increased (Figure 1) [1, 33]. Recently, Lin *et al* reported increased GFP and AMPA receptor expression under mild hypothermia conditions [34]. With recent increases in cryoEM studies it is also foreseeable that mammalian cell expression will increase since considerably less material is required compared to crystallographic studies.

Baculovirus mediated gene transduction of mammalian cells (BacMam) has been widely used due to its compatibility with a variety of mammalian cell lines, the possibility of co-infecting with multiple BacMam viruses to express protein complexes and its rapid and efficient target over expression [9, 35]. Furthermore, recent modifications of the BacMam system allow for assembly of multiple expression cassettes and, by taking advantage of having GFP fusion constructs of the target proteins, high throughput screening of constructs by small-scale transfection/FSEC before moving to large-scale protein expression [9].

Cell free

Cell-free protein expression is a rapid method for synthesis of recombinant proteins that uses cell lysates as the source of the whole protein translational machinery. The cell lysate can be derived from a variety of sources ranging in complexity from bacterial to mammalian systems each attempting native lipidation, glycosylation, phosphorylation and other PTMs [36]. Providing modifying enzymes can in principle make PTMs possible even in *E. coli*, however the quality and homogeneity of PTMs is unlikely to be sufficient for downstream structural studies [37].

Pre-expression strategies

The screening of a range of orthologues should be carried out to identify a promising starting target. However, this alone is normally not enough to lead to a structure, and additional testing and modification needed. In the last two years only ~12% of recombinant eIMP structures were solved with the native full-length sequence (Supplementary Table 1 and Supplementary Figure 3). In recent years the trend has been to modify the protein construct before structural studies. Such modifications can be classified broadly as pre-expression and post-expression, and will be described in the coming sections.

Pre-expression modifications comprise a range of strategies that directly alter the gene of interest in an effort to improve the conformational/thermo-stability and/or "crystallizability" of the expressed protein. These strategies include the addition of point mutations to 1) improve protein stability 2) remove post-translational modification sites and 3) alter the surface properties of the protein, as well, as the truncation of disordered termini and loops or their substitution by ordered fusion proteins such as T4 lysozyme (T4L) and cytochrome b_{562} RIL (BRIL) [38, 39].

Construct design for structural studies

Conformational/Thermo stabilisation

Thermostabilisation involves the systematic screening of point mutations (typically alanine) that translate to an increase in the protein 'melting temperature' as determined by a radioligand binding or a fluorescent thermostability assay. These mutations often render the protein inactive or locked in a discrete conformation, and therefore an assay based on a proper enzymatic activity may not be amenable. In the last two years, ~14% of the eIMP structures determined have involved the inclusion of thermostabilising mutations (Supplementary Table 1 and Supplementary Figure 3). However, the process to identify thermostabilising mutations can be quite cumbersome especially for larger proteins. Experimentally, this can be partly overcome by either limiting mutational space [40, 41] or through the use of high-throughput methods [42-44]. Alternatively, *in silico* stability calculations and sequence conservation may offer some guidance [45] but often require *a priori* knowledge, which obviously is not available to novel, unknown structures. Recently, Sauer *et al*. reported two different multiple sequence analysis methodologies to identify potentially thermostabilising mutations, centred on a rationalisation of a correlation between an organism's optimum growth temperature and protein stability [46]. These results lend hope that rational strategies can be devised to facilitate the process.

Protein engineering

Another common strategy to generate a stable target for structural studies is the truncation of the termini and loop regions, focussing on disordered regions that can potentially affect crystal packing or promote protein aggregation (Supplementary Table 1 and Supplementary Figure 3). Useful sites for truncation can be identified experimentally through limited proteolysis, or *in silico*[47] using sequence alignments and a number of online tools, which serve to either predict regions of conserved special features (secondary structure, transmembrane topology[48] and domains[49]) or disordered regions within protein sequences[50, 51].

An alternative to the truncation of a disordered protein region is to replace it with a suitable fusion protein. Solutions currently in fashion include the stabilised BRIL and T4L moieties, which in the GPCR field are used to typically replace intracellular loop 3 of the receptor[38, 39]. In addition to an overall stabilising effect on the protein these fusions can also play a role in the formation of crystal contacts. Recently, Yin *et al*. introduced a novel fusion protein in the structure determination of the human OX2 receptor, namely the catalytic domain of the *Pyrococcus abysii* glycogen synthase[52]. The generation of chimeras from domains of related proteins represents an alternative approach to thermostabilisation and can provide a unique source for crystal contacts[53-56].

Webservers can also be used to predict a range of PTM sites, for mutagenesis [57]. In addition, webservers also allow for the identification of residues for mutation to lower the surface entropy of the target protein promoting more favourable interactions for crystallisation [58].

Purification tags

For many, the workhorse poly-histidine tag remains the purification strategy of choice for eIMPs irrespective of expression system (Figure 2a). However, in the case of the higher eukaryote expression systems, such as HEK cells, the use of the more specific cobalt charged IMAC resin is often preferred over traditional nickel-NTA resin, due in part to the expanded range of sequences that can bind Ni-NTA. Alternatively, protein affinity tags (StrepII) or antibody affinity tags (FLAG and 1D4) offer an additional advantage of increased specificity and remain an attractive option for instances of low expression.

Post-expression strategies

Post-expression strategies cover a range of approaches that can be applied to the protein of interest before and during purification. They include the use of small molecules (ligand, inhibitors, lipids) or proteins (nanobodies, antibodies) to stabilise the target protein in a given conformation and represent a common strategy for receptors and transporters [59]. The add-back of native and non-native lipids during purification serves to offset the delipidation of the protein target during subsequent chromatography, thus increasing stability. In addition, surface modification of the protein by alkylation of free cysteines or the reductive methylation of lysine can also be exploited to modify the solution properties of the target.

Enzymatic treatment of the protein to remove PTMs or disordered regions (limited proteolysis) can be employed to generate a more homogenous protein sample [59].

These enzymatic approaches would be advisable if mutation of PTM sites or truncation of disordered regions lead to lower expression levels than that of the mature full-length protein. The efficiency of limited proteolysis can be improved by the introduction of a specific protease site in the region of interest[60].

Detergents

The choice of detergent is central to the success of structural and functional studies of IMPs [61]. However, choosing a detergent is largely empirical, which can be further complicated as the optimal solubilisation detergent is often not compatible with structure determination. GFP-fusion constructs offer a high-throughput tool amenable for the rapid screening of detergents at various stages of the solubilisation and purification pipeline [8, 42]. Recently, methods for the characterisation of protein detergent complexes have been reported centred on multiple detections during size exclusion chromatography [62, 63].

Dodecyl-B-D-maltoside (DDM) and a combination of DDM and cholesteryl hemisuccinate (CHS) represent the solubilisation detergent compositions of choice for ~45% of the structures solved in the past two years, dropping to 30% for the purification/structure solution detergent compositions (Figure 3a and b, Supplementary Table 1). In the case of the latter, the detergent choice tends towards those with low critical micelle concentrations or smaller micelles (Figure 3b, Supplementary Table 1).

Alternative approaches to protein reconstitution have been described including saposin lipoprotein nanoparticles and styrene maleic acid co-polymer lipid particles (SMALPs) that have the potential to provide a detergent free approach in IMP structure determination, especially by cryo-EM [64-67].

Crystallisation

X-ray diffraction remains the most dominant method for eIMP structure determination over the past 2 years (Figure 3b). Detergent-based methods are still the dominant approach for the crystallization of eIMPs (Figure 3c). The purified detergent-solubilized protein is used directly in crystallization trials using conventional vapor diffusion, dialysis and microbatch methods. However, detergents do not mimic the native lipid bilayer and can cover most of the protein surface area available for crystal contacts [68]. While the latter can be offset using shorter chained detergents, these often destabilise the protein of interest[69], not least eIMPs.

Addition and control of lipids can play a key role in improving crystal packing. The protein sample can be re-lipidated throughout purification and crystallization to obtain crystals such as for the *Drosophila melanogaster* dopamine transporter that was re-lipidated prior to crystallization [70], or by using the high-lipid high-detergent approach (HiLiDe) [71-74]. The HiLiDe method, inspired by detergent solubilization of enriched microsomes from native sources (e.g., pig kidney Na,K-ATPase and rabbit fast-twitch muscle SERCA1a, Figure 3c and Supplementary Table 1), utilizes overnight mixing of extra lipid and/or detergent with the purified protein sample [75, 76]. A mild lipid exchange can be obtained by ultracentrifugation in sucrose gradients, where specific lipid/cholesterol compositions can be obtained without

going through de-lipidating steps or demanding chromatography in lipidated buffers [76].

Another lipid based crystallisation method is the lipidic cubic phase (LCP) method [77], which has been essential for the structure determination of GPCRs [78] including the engineered rhodopsin-arrestin complex[79], and also non-GPCRs such as the human glucose transporter GLUT3 [80] the vacuolar H^+/Ca^{2+} exchanger (VCX1) [81] and prostaglandin E2 synthase [56] (Supplementary Table 1, Figure 3c).

The third lipid-based crystallization method is the bicelle method [82, 83]. Bicelles are membrane mimetic systems comprising of lipid bilayer disks that are formed in certain lipid/amphiphile mixtures, and shares characteristics with LCP and HILIDE. Recently, the structure of voltage dependent anion channel 1 (VDAC1) has been determined from bicelle grown crystals [84].

Conclusions and perspectives

The structural studies of eIMPs is a largely empirical process. While some degrees of bias exist in the data presented here, i.e. GPCRs represent 22% of the entries, clear trends in the choice of expression system and the design of constructs are noted from the analysis of successes over the past two years. This involves the screening of a range of orthologues in the chosen expression system, with the caveat that success for mammalian genes is more probable when using a more complex expression system. For crystal based structural studies, pre- and post-expression modification of the target increases the chances of success. This can be hallmarked by the revolution in GPCR structural biology that has been driven in large by the establishment of a number of pipelines that combine many pre- and post expression strategies required for success. Expression modifications may on the other hand be less critical for cryoEM. These strategies will be critical for success in the future studies of the many eIMPs that remain of unknown structure and function, and the higher-order complexes in biomembranes.

Figure Legends

Figure 1: Distribution of expression systems for (a) eukaryotic, (b) mammalian and (c) human integral membrane proteins over the past 2 years. Values for each entry are indicated over the respective bar. See Supplementary Table 1 for a detailed description of selection criteria.

Figure 2: (a) Purification strategy, (b) experimental methods used for structure determination and (c) crystallisation methods used for eukaryotic membrane proteins over the last 2 years. Inset summarises the breakdown of usage for the polyHis, FLAG and StrepII entries in (a), respectively. Total values for each entry are indicated over the respective bar. For a detailed description of selection criteria see Supplementary Table 1.

Figure 3: Detergents used in a) solubilisation and b) purification of eukaryotic membrane proteins over the last 2 years. Expression systems are indicated as Native (orange), bacterial and yeast (green) and insect and mammalian (blue). Data are shown for entries where n>/=2. Total values for each entry are indicated over the respective bar. For a detailed description of selection criteria and list of abbreviations see Supplementary Table 1 and Supplementary Figure 2 for the complete chart.

Supplementary Figure 1: Distribution of source organism for genes resulting in eukaryotic integral membrane protein structures over the past 2 years. Values for each entry are indicated over the respective bar.

Supplementary Figure 2: Detergents used in a) solubilisation and b) purification of eukaryotic membrane proteins over the last 2 years. Expression systems are indicated as Native (orange), bacterial and yeast (green) and insect and mammalian (blue). Total values for each entry are indicated over the respective bar. For a detailed description of selection criteria and list of abbreviations see Supplementary Table 1. Abbreviations

Supplementary Figure 3: Pre- and post expression strategies used for the structure determination of eukaryotic membrane proteins over the last 2 years. Values for each entry are indicated over the respective bar. For a detailed description of selection criteria see Supplementary Table 1.

References:

1. Andrell, J. and C.G. Tate, *Overexpression of membrane proteins in mammalian cells for structural studies*. Mol Membr Biol, 2013. **30**(1): p. 52-63.
2. Fan, G., M.L. Baker, Z. Wang, M.R. Baker, P.A. Sinyagovskiy, W. Chiu, S.J. Ludtke, and Serysheva, II, *Gating machinery of InsP3R channels revealed by electron cryomicroscopy*. Nature, 2015. **527**(7578): p. 336-41.
3. Zalk, R., O.B. Clarke, A. des Georges, R.A. Grassucci, S. Reiken, F. Mancia, W.A. Hendrickson, J. Frank, and A.R. Marks, *Structure of a mammalian ryanodine receptor*. Nature, 2015. **517**(7532): p. 44-9.
4. Yan, Z., X.C. Bai, C. Yan, J. Wu, Z. Li, T. Xie, W. Peng, C.C. Yin, X. Li, S.H. Scheres, Y. Shi, and N. Yan, *Structure of the rabbit ryanodine receptor RyR1 at near-atomic resolution*. Nature, 2015. **517**(7532): p. 50-5.
5. Wu, J., Z. Yan, Z. Li, C. Yan, S. Lu, M. Dong, and N. Yan, *Structure of the voltage-gated calcium channel Cav1.1 complex*. Science, 2015. **350**(6267): p. aad2395.
6. Brooks, C.L., M. Morrison, and M. Joanne Lemieux, *Rapid expression screening of eukaryotic membrane proteins in Pichia pastoris*. Protein Sci, 2013. **22**(4): p. 425-33.
7. Newstead, S., H. Kim, G. von Heijne, S. Iwata, and D. Drew, *High-throughput fluorescent-based optimization of eukaryotic membrane protein overexpression and purification in Saccharomyces cerevisiae*. Proc Natl Acad Sci U S A, 2007. **104**(35): p. 13936-41.
8. Drew, D., S. Newstead, Y. Sonoda, H. Kim, G. von Heijne, and S. Iwata, *GFP-based optimization scheme for the overexpression and purification of eukaryotic membrane proteins in Saccharomyces cerevisiae*. Nat Protoc, 2008. **3**(5): p. 784-98.
9. Goehring, A., C.H. Lee, K.H. Wang, J.C. Michel, D.P. Claxton, I. Baconguis, T. Althoff, S. Fischer, K.C. Garcia, and E. Gouaux, *Screening and large-scale expression of membrane proteins in mammalian cells for structural studies*. Nat Protoc, 2014. **9**(11): p. 2574-85.
10. Drew, D., M. Lerch, E. Kunji, D.J. Slotboom, and J.W. de Gier, *Optimization of membrane protein overexpression and purification using GFP fusions*. Nat Methods, 2006. **3**(4): p. 303-13.
11. Drew, D.E., G. von Heijne, P. Nordlund, and J.W. de Gier, *Green fluorescent protein as an indicator to monitor membrane protein overexpression in Escherichia coli*. FEBS Lett, 2001. **507**(2): p. 220-4.
12. Khow, O. and S. Suntrarachun, *Strategies for production of active eukaryotic proteins in bacterial expression system*. Asian Pac J Trop Biomed, 2012. **2**(2): p. 159-62.
13. Long, S.B., E.B. Campbell, and R. Mackinnon, *Crystal structure of a mammalian voltage-dependent Shaker family K+ channel*. Science, 2005. **309**(5736): p. 897-903.
14. Jidenko, M., R.C. Nielsen, T.L. Sorensen, J.V. Moller, M. le Maire, P. Nissen, and C. Jaxel, *Crystallization of a mammalian membrane protein overexpressed in Saccharomyces cerevisiae*. Proc Natl Acad Sci U S A, 2005. **102**(33): p. 11687-91.
15. Byrne, B., *Pichia pastoris as an expression host for membrane protein structural biology*. Curr Opin Struct Biol, 2015. **32**: p. 9-17.

Comment [lyons1]: **

Comment [lyons2]: **

Comment [lyons3]: **

Comment [lyons4]: **

16. Macauley-Patrick, S., M.L. Fazenda, B. McNeil, and L.M. Harvey, *Heterologous protein production using the Pichia pastoris expression system*. Yeast, 2005. **22**(4): p. 249-70.
17. Mizutani, K., S. Yoshioka, Y. Mizutani, S. Iwata, and B. Mikami, *High-throughput construction of expression system using yeast Pichia pastoris, and its application to membrane proteins*. Protein Expr Purif, 2011. **77**(1): p. 1-8.
18. Murray, J.A., *Bending the rules: the 2-mu plasmid of yeast*. Mol Microbiol, 1987. **1**(1): p. 1-4.
19. Erhart, E. and C.P. Hollenberg, *The presence of a defective LEU2 gene on 2 mu DNA recombinant plasmids of Saccharomyces cerevisiae is responsible for curing and high copy number*. J Bacteriol, 1983. **156**(2): p. 625-35.
20. Parker, J.L. and S. Newstead, *Method to increase the yield of eukaryotic membrane protein expression in Saccharomyces cerevisiae for structural and functional studies*. Protein Sci, 2014. **23**(9): p. 1309-14.
21. Bomholt, J., C. Helix-Nielsen, P. Scharff-Poulsen, and P.A. Pedersen, *Recombinant production of human Aquaporin-1 to an exceptional high membrane density in Saccharomyces cerevisiae*. PLoS One, 2013. **8**(2): p. e56431.
22. Ciccarone, V.C., D.A. Polayes, and V.A. Luckow, *Generation of Recombinant Baculovirus DNA in E.coli Using a Baculovirus Shuttle Vector*. Methods Mol Med, 1998. **13**: p. 213-35.
23. Contreras-Gomez, A., A. Sanchez-Miron, F. Garcia-Camacho, E. Molina-Grima, and Y. Chisti, *Protein production using the baculovirus-insect cell expression system*. Biotechnol Prog, 2014. **30**(1): p. 1-18.
24. Bieniossek, C., T.J. Richmond, and I. Berger, *MultiBac: multigene baculovirus-based eukaryotic protein complex production*. Curr Protoc Protein Sci, 2008. **Chapter 5**: p. Unit 5 20.
25. Bieniossek, C., T. Imasaki, Y. Takagi, and I. Berger, *MultiBac: expanding the research toolbox for multiprotein complexes*. Trends Biochem Sci, 2012. **37**(2): p. 49-57.
26. Fitzgerald, D.J., P. Berger, C. Schaffitzel, K. Yamada, T.J. Richmond, and I. Berger, *Protein complex expression by using multigene baculoviral vectors*. Nat Methods, 2006. **3**(12): p. 1021-32.
27. Siupka, P., O.T. Hamming, L. Kang, H.H. Gad, and R. Hartmann, *A conserved sugar bridge connected to the WSXWS motif has an important role for transport of IL-21R to the plasma membrane*. Genes Immun, 2015. **16**(6): p. 405-13.
28. Jarvis, D.L., *Developing baculovirus-insect cell expression systems for humanized recombinant glycoprotein production*. Virology, 2003. **310**(1): p. 1-7.
29. Geisler, C. and D.L. Jarvis, *Innovative use of a bacterial enzyme involved in sialic acid degradation to initiate sialic acid biosynthesis in glycoengineered insect cells*. Metab Eng, 2012. **14**(6): p. 642-52.
30. Hollister, J., E. Grabenhorst, M. Nimtz, H. Conradt, and D.L. Jarvis, *Engineering the protein N-glycosylation pathway in insect cells for production of biantennary, complex N-glycans*. Biochemistry, 2002. **41**(50): p. 15093-104.
31. Zhu, J., *Mammalian cell protein expression for biopharmaceutical production*. Biotechnol Adv, 2012. **30**(5): p. 1158-70.
32. Sunley, K. and M. Butler, *Strategies for the enhancement of recombinant protein production from mammalian cells by growth arrest*. Biotechnol Adv, 2010. **28**(3): p. 385-94.

33. He, Y., K. Wang, and N. Yan, *The recombinant expression systems for structure determination of eukaryotic membrane proteins*. Protein Cell, 2014. **5**(9): p. 658-72.
34. Lin, C.Y., Z. Huang, W. Wen, A. Wu, C. Wang, and L. Niu, *Enhancing Protein Expression in HEK-293 Cells by Lowering Culture Temperature*. PLoS One, 2015. **10**(4): p. e0123562.
35. Dukkipati, A., H.H. Park, D. Waghray, S. Fischer, and K.C. Garcia, *BacMam system for high-level expression of recombinant soluble and membrane glycoproteins for structural studies*. Protein Expr Purif, 2008. **62**(2): p. 160-70.
36. Zemella, A., L. Thoring, C. Hoffmeister, and S. Kubick, *Cell-Free Protein Synthesis: Pros and Cons of Prokaryotic and Eukaryotic Systems*. Chembiochem, 2015. **16**(17): p. 2420-31.
37. Guarino, C. and M.P. DeLisa, *A prokaryote-based cell-free translation system that efficiently synthesizes glycoproteins*. Glycobiology, 2012. **22**(5): p. 596-601.
38. Rosenbaum, D.M., V. Cherezov, M.A. Hanson, S.G. Rasmussen, F.S. Thian, T.S. Kobilka, H.J. Choi, X.J. Yao, W.I. Weis, R.C. Stevens, and B.K. Kobilka, *GPCR engineering yields high-resolution structural insights into beta2-adrenergic receptor function*. Science, 2007. **318**(5854): p. 1266-73.
39. Chun, E., A.A. Thompson, W. Liu, C.B. Roth, M.T. Griffith, V. Katritch, J. Kunken, F. Xu, V. Cherezov, M.A. Hanson, and R.C. Stevens, *Fusion partner toolchest for the stabilization and crystallization of G protein-coupled receptors*. Structure, 2012. **20**(6): p. 967-76.
40. Serrano-Vega, M.J., F. Magnani, Y. Shibata, and C.G. Tate, *Conformational thermostabilization of the beta1-adrenergic receptor in a detergent-resistant form*. Proc Natl Acad Sci U S A, 2008. **105**(3): p. 877-82.
41. Abdul-Hussein, S., J. Andrell, and C.G. Tate, *Thermostabilisation of the serotonin transporter in a cocaine-bound conformation*. J Mol Biol, 2013. **425**(12): p. 2198-207.
42. Hattori, M., R.E. Hibbs, and E. Gouaux, *A fluorescence-detection size-exclusion chromatography-based thermostability assay for membrane protein precrystallization screening*. Structure, 2012. **20**(8): p. 1293-9.
43. Asial, I., Y.X. Cheng, H. Engman, M. Dollhopf, B. Wu, P. Nordlund, and T. Cornvik, *Engineering protein thermostability using a generic activity-independent biophysical screen inside the cell*. Nat Commun, 2013. **4**: p. 2901.
44. Sarkar, C.A., I. Dodevski, M. Kenig, S. Dudli, A. Mohr, E. Hermans, and A. Pluckthun, *Directed evolution of a G protein-coupled receptor for expression, stability, and binding selectivity*. Proc Natl Acad Sci U S A, 2008. **105**(39): p. 14808-13.
45. Bhattacharya, S., S. Lee, R. Grisshammer, C.G. Tate, and N. Vaidehi, *Rapid Computational Prediction of Thermostabilizing Mutations for G Protein-Coupled Receptors*. J Chem Theory Comput, 2014. **10**(11): p. 5149-5160.
46. Sauer, D.B., N.K. Karpowich, J.M. Song, and D.N. Wang, *Rapid Bioinformatic Identification of Thermostabilizing Mutations*. Biophys J, 2015. **109**(7): p. 1420-8.
47. Mooij, W.T., E. Mitsiki, and A. Perrakis, *ProteinCCD: enabling the design of protein truncation constructs for expression and crystallization experiments*. Nucleic Acids Res, 2009. **37**(Web Server issue): p. W402-5.
48. Kall, L., A. Krogh, and E.L. Sonnhammer, *Advantages of combined transmembrane topology and signal peptide prediction--the Phobius web server*. Nucleic Acids Res, 2007. **35**(Web Server issue): p. W429-32.

Comment [lyons5]: *

49. Letunic, I., R.R. Copley, B. Pils, S. Pinkert, J. Schultz, and P. Bork, *SMART 5: domains in the context of genomes and networks*. Nucleic Acids Res, 2006. **34**(Database issue): p. D257-60.
50. Yang, Z.R., R. Thomson, P. McNeil, and R.M. Esnouf, *RONN: the bio-basis function neural network technique applied to the detection of natively disordered regions in proteins*. Bioinformatics, 2005. **21**(16): p. 3369-76.
51. Jones, D.T. and D. Cozzetto, *DISOPRED3: precise disordered region predictions with annotated protein-binding activity*. Bioinformatics, 2015. **31**(6): p. 857-63.
52. Yin, J., J.C. Mobarec, P. Kolb, and D.M. Rosenbaum, *Crystal structure of the human OX2 orexin receptor bound to the insomnia drug suvorexant*. Nature, 2015. **519**(7542): p. 247-50.
53. Takeshita, K., S. Sakata, E. Yamashita, Y. Fujiwara, A. Kawanabe, T. Kurokawa, Y. Okochi, M. Matsuda, H. Narita, Y. Okamura, and A. Nakagawa, *X-ray crystal structure of voltage-gated proton channel*. Nat Struct Mol Biol, 2014. **21**(4): p. 352-7.
54. Kato, H.E., M. Kamiya, S. Sugo, J. Ito, R. Taniguchi, A. Orito, K. Hirata, A. Inutsuka, A. Yamanaka, A.D. Maturana, R. Ishitani, Y. Sudo, S. Hayashi, and O. Nureki, *Atomistic design of microbial opsin-based blue-shifted optogenetics tools*. Nat Commun, 2015. **6**: p. 7177.
55. Ahuja, S., S. Mukund, L. Deng, K. Khakh, E. Chang, H. Ho, S. Shriver, C. Young, S. Lin, J.P. Johnson, Jr., P. Wu, J. Li, M. Coons, C. Tam, B. Brillantes, H. Sampang, K. Mortara, K.K. Bowman, K.R. Clark, A. Estevez, Z. Xie, H. Verschoof, M. Grimwood, C. Dehnhardt, J.C. Andrez, T. Focken, D.P. Sutherlin, B.S. Safina, M.A. Starovasnik, D.F. Ortwine, Y. Franke, C.J. Cohen, D.H. Hackos, C.M. Koth, and J. Payandeh, *Structural basis of Nav1.7 inhibition by an isoform-selective small-molecule antagonist*. Science, 2015. **350**(6267): p. aac5464.
56. Li, D., N. Howe, A. Dukkipati, S.T. Shah, B.D. Bax, C. Edge, A. Bridges, P. Hardwicke, O.M. Singh, G. Giblin, A. Pautsch, R. Pfau, G. Schnapp, M. Wang, V. Olieric, and M. Caffrey, *Crystallizing Membrane Proteins in the Lipidic Mesophase. Experience with Human Prostaglandin E2 Synthase 1 and an Evolving Strategy*. Cryst Growth Des, 2014. **14**(4): p. 2034-2047.
57. Eisenhaber, B. and F. Eisenhaber, *Prediction of posttranslational modification of proteins from their amino acid sequence*. Methods Mol Biol, 2010. **609**: p. 365-84.
58. Goldschmidt, L., D.R. Cooper, Z.S. Derewenda, and D. Eisenberg, *Toward rational protein crystallization: A Web server for the design of crystallizable protein variants*. Protein Sci, 2007. **16**(8): p. 1569-76.
59. Columbus, L., *Post-expression strategies for structural investigations of membrane proteins*. Curr Opin Struct Biol, 2015. **32**: p. 131-8.
60. Penmatsa, A., K.H. Wang, and E. Gouaux, *X-ray structures of Drosophila dopamine transporter in complex with nisoxetine and reboxetine*. Nat Struct Mol Biol, 2015. **22**(6): p. 506-8.
61. Thomas, J. and C.G. Tate, *Quality control in eukaryotic membrane protein overproduction*. J Mol Biol, 2014. **426**(24): p. 4139-54.
62. Miercke, L.J., R.A. Robbins, and R.M. Stroud, *Tetra detector analysis of membrane proteins*. Curr Protoc Protein Sci, 2014. **77**: p. 29 10 1-30.
63. Gimpl, K., J. Klement, and S. Keller, *Characterising protein/detergent complexes by triple-detection size-exclusion chromatography*. Biol Proced Online, 2016. **18**: p. 4.
64. Frauenfeld, J., R. Loving, J.P. Armache, A.F. Sonnen, F. Guettou, P. Moberg, L. Zhu, C. Jegerschold, A. Flayhan, J.A. Briggs, H. Garoff, C. Low, Y. Cheng, and P. Nordlund,

Comment [lyons6]: *

Comment [lyons7]: *

A saposin-lipoprotein nanoparticle system for membrane proteins. Nat Methods, 2016. **13**(4): p. 345-51.
65. Postis, V., S. Rawson, J.K. Mitchell, S.C. Lee, R.A. Parslow, T.R. Dafforn, S.A. Baldwin, and S.P. Muench, *The use of SMALPs as a novel membrane protein scaffold for structure study by negative stain electron microscopy*. Biochim Biophys Acta, 2015. **1848**(2): p. 496-501.
66. Dorr, J.M., S. Scheidelaar, M.C. Koorengevel, J.J. Dominguez, M. Schafer, C.A. van Walree, and J.A. Killian, *The styrene-maleic acid copolymer: a versatile tool in membrane research*. Eur Biophys J, 2016. **45**(1): p. 3-21.
67. Lee, S.C., S. Khalid, N.L. Pollock, T.J. Knowles, K. Edler, A.J. Rothnie, R.T.T. O, and T.R. Dafforn, *Encapsulated membrane proteins: A simplified system for molecular simulation*. Biochim Biophys Acta, 2016.
68. Michel, H., *Crystallization of membrane proteins*. Trends in Biochemical Sciences, 1983. **8**(2): p. 56-59.
69. Tate, C.G., *Practical considerations of membrane protein instability during purification and crystallisation*. Methods Mol Biol, 2010. **601**: p. 187-203.
70. Wang, K.H., A. Penmatsa, and E. Gouaux, *Neurotransmitter and psychostimulant recognition by the dopamine transporter*. Nature, 2015. **521**(7552): p. 322-7.
71. Sitsel, O., K. Wang, X. Liu, and P. Gourdon, *Crystallization of P-type ATPases by the High Lipid-Detergent (HiLiDe) Method*. Methods Mol Biol, 2016. **1377**: p. 413-20.
72. Gourdon, P., J.L. Andersen, K.L. Hein, M. Bublitz, B.P. Pedersen, X.-Y. Liu, L. Yatime, M. Nyblom, T.T. Nielsen, C. Olesen, J.V. Møller, P. Nissen, and J.P. Morth, *HiLiDe—Systematic Approach to Membrane Protein Crystallization in Lipid and Detergent*. Crystal Growth & Design, 2011. **11**(6): p. 2098-2106.
73. Malinauskaite, L., M. Quick, L. Reinhard, J.A. Lyons, H. Yano, J.A. Javitch, and P. Nissen, *A mechanism for intracellular release of Na+ by neurotransmitter/sodium symporters*. Nat Struct Mol Biol, 2014. **21**(11): p. 1006-12.
74. Chen, L., K.L. Dürr, and E. Gouaux, *X-ray structures of AMPA receptor–cone snail toxin complexes illuminate activation mechanism*. Science, 2014. **345**(6200): p. 1021-1026.
75. Laursen, M., J.L. Gregersen, L. Yatime, P. Nissen, and N.U. Fedosova, *Structures and characterization of digoxin- and bufalin-bound Na+,K+-ATPase compared with the ouabain-bound complex*. Proc Natl Acad Sci U S A, 2015. **112**(6): p. 1755-60.
76. Drachmann, N.D., C. Olesen, J.V. Moller, Z. Guo, P. Nissen, and M. Bublitz, *Comparing crystal structures of Ca(2+) -ATPase in the presence of different lipids*. FEBS J, 2014. **281**(18): p. 4249-62.
77. Caffrey, M., *A comprehensive review of the lipid cubic phase or in meso method for crystallizing membrane and soluble proteins and complexes*. Acta Crystallogr F Struct Biol Commun, 2015. **71**(Pt 1): p. 3-18.
78. Yin, X., H. Xu, M. Hanson, and W. Liu, *GPCR crystallization using lipidic cubic phase technique*. Curr Pharm Biotechnol, 2014. **15**(10): p. 971-9.
79. Kang, Y., X.E. Zhou, X. Gao, Y. He, W. Liu, A. Ishchenko, A. Barty, T.A. White, O. Yefanov, G.W. Han, Q. Xu, P.W. de Waal, J. Ke, M.H. Tan, C. Zhang, A. Moeller, G.M. West, B.D. Pascal, N. Van Eps, L.N. Caro, S.A. Vishnivetskiy, R.J. Lee, K.M. Suino-Powell, X. Gu, K. Pal, J. Ma, X. Zhi, S. Boutet, G.J. Williams, M. Messerschmidt, C. Gati, N.A. Zatsepin, D. Wang, D. James, S. Basu, S. Roy-Chowdhury, C.E. Conrad, J. Coe, H. Liu, S. Lisova, C. Kupitz, I. Grotjohann, R. Fromme, Y. Jiang, M. Tan, H. Yang, J. Li, M. Wang, Z. Zheng, D. Li, N. Howe, Y. Zhao, J. Standfuss, K. Diederichs, Y. Dong, C.S. Potter, B. Carragher, M. Caffrey, H. Jiang, H.N. Chapman, J.C. Spence, P.

Comment [lyons8]: **

Comment [lyons9]: **

Fromme, U. Weierstall, O.P. Ernst, V. Katritch, V.V. Gurevich, P.R. Griffin, W.L. Hubbell, R.C. Stevens, V. Cherezov, K. Melcher, and H.E. Xu, *Crystal structure of rhodopsin bound to arrestin by femtosecond X-ray laser*. Nature, 2015. **523**(7562): p. 561-7.
80. Deng, D., P. Sun, C. Yan, M. Ke, X. Jiang, L. Xiong, W. Ren, K. Hirata, M. Yamamoto, S. Fan, and N. Yan, *Molecular basis of ligand recognition and transport by glucose transporters*. Nature, 2015. **526**(7573): p. 391-6.
81. Waight, A.B., B.P. Pedersen, A. Schlessinger, M. Bonomi, B.H. Chau, Z. Roe-Zurz, A.J. Risenmay, A. Sali, and R.M. Stroud, *Structural basis for alternating access of a eukaryotic calcium/proton exchanger*. Nature, 2013. **499**(7456): p. 107-10.
82. Poulos, S., J.L. Morgan, J. Zimmer, and S. Faham, *Bicelles coming of age: an empirical approach to bicelle crystallization*. Methods Enzymol, 2015. **557**: p. 393-416.
83. Faham, S. and J.U. Bowie, *Bicelle crystallization: a new method for crystallizing membrane proteins yields a monomeric bacteriorhodopsin structure*. J Mol Biol, 2002. **316**(1): p. 1-6.
84. Choudhary, O.P., A. Paz, J.L. Adelman, J.P. Colletier, J. Abramson, and M. Grabe, *Structure-guided simulations illuminate the mechanism of ATP transport through VDAC1*. Nat Struct Mol Biol, 2014. **21**(7): p. 626-32.

Acknowledgements
This was work was supported by postdoctoral fellowship R171-2014-663 from the Lundbeck Foundation (to J.L.), a fellowship from the Aarhus Institute of Advanced Studies (to B.P.P.), and a Sapere Aude research grant from the Danish Council for Independent Research (to B.P.P.).

Figure 1

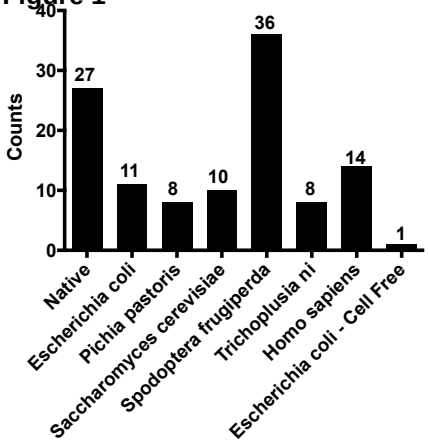
Counts
40
30
20
10
0
27
11
8
10
36
8
14
1
Native
Escherichia coli
Pichia pastoris
Saccharomyces cerevisiae
Spodoptera frugiperda
Trichoplusia ni
Homo sapiens
Escherichia coli - Cell Free

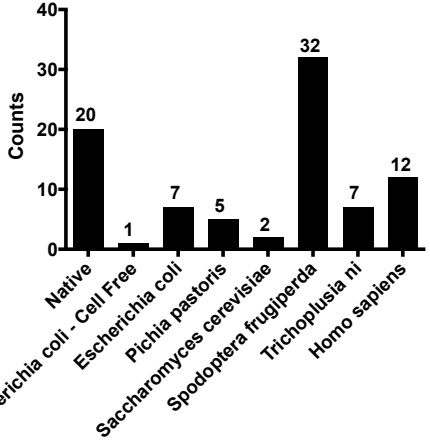
Counts
40
30
20
10
0
20
1
7
5
2
32
7
12
Native
Escherichia coli - Cell Free
Escherichia coli
Pichia pastoris
Saccharomyces cerevisiae
Spodoptera frugiperda
Trichoplusia ni
Homo sapiens

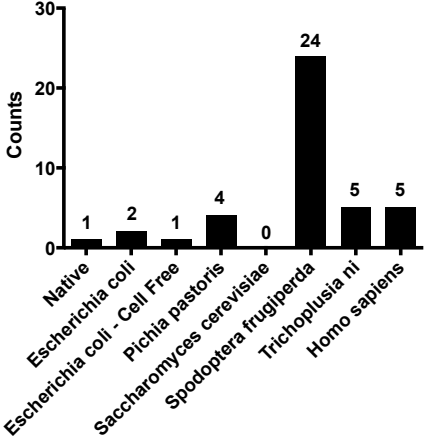
Counts
30
20
10
0
1
2
1
4
0
24
5
5
Native
Escherichia coli
Escherichia coli - Cell Free
Pichia pastoris
Saccharomyces cerevisiae
Spodoptera frugiperda
Trichoplusia ni
Homo sapiens

Figure 2

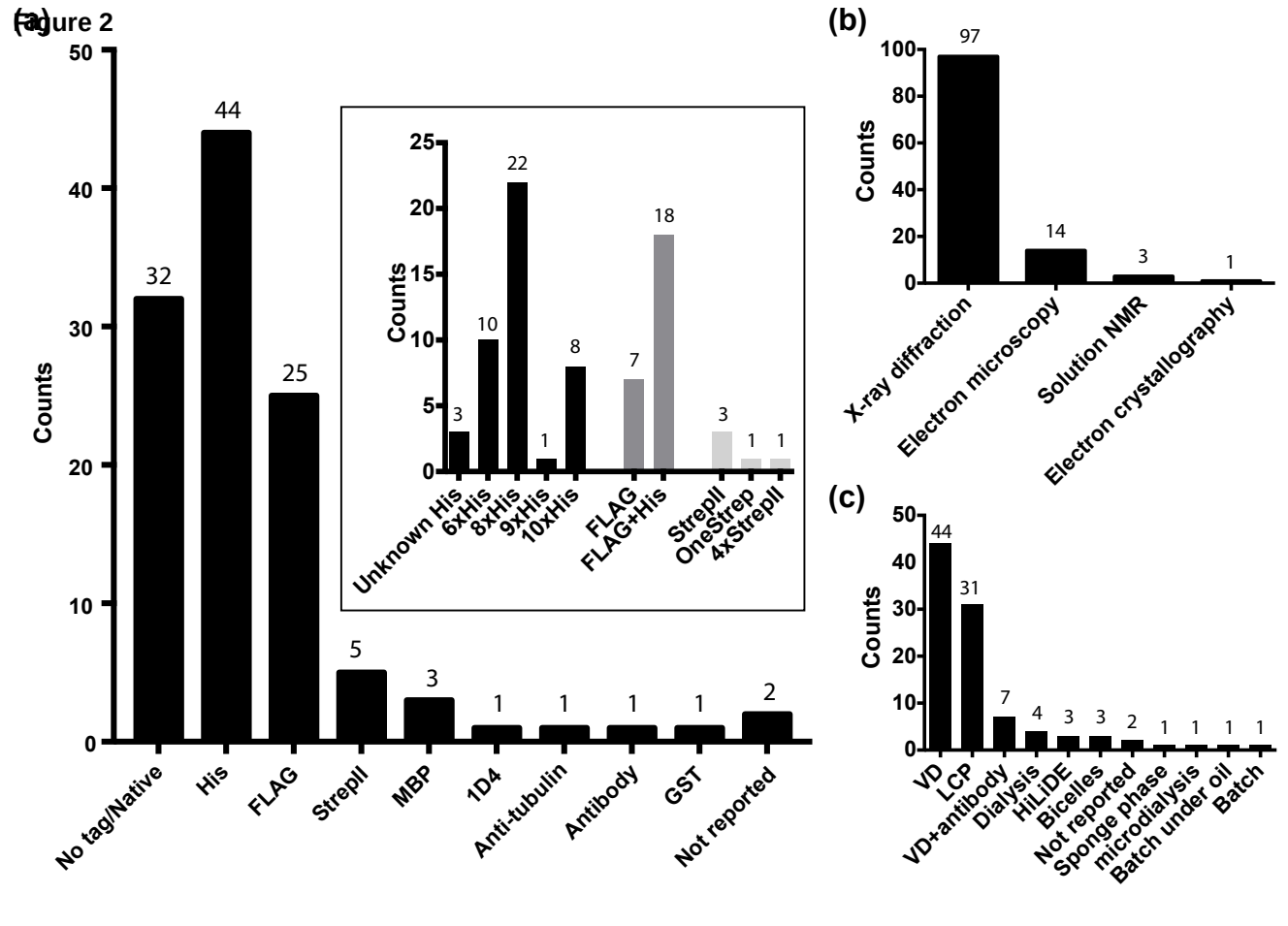
(a)
Counts
50
40
30
20
10
0
32
44
25
5
3
1
1
1
1
2
No tag/Native
His
FLAG
StrepII
MBP
1D4
Anti-tubulin
Antibody
GST
Not reported
Counts
25
20
15
10
5
0
3
10
22
1
8
7
18
3
1
1
Unknown His
6xHis
8xHis
9xHis
10xHis
FLAG
FLAG+His
StrepII
OneStrep
4xStrepII
(b)
Counts
100
80
60
40
20
0
97
14
3
1
X-ray diffraction
Electron microscopy
Solution NMR
Electron crystallography
(c)
Counts
50
40
30
20
10
0
44
31
7
4
3
3
2
1
1
1
1
VD
LCP
VD+antibody
Dialysis
HiLiDE
Bicelles
Not reported
Sponge phase
microdialysis
Batch under oil
Batch

Figure 3

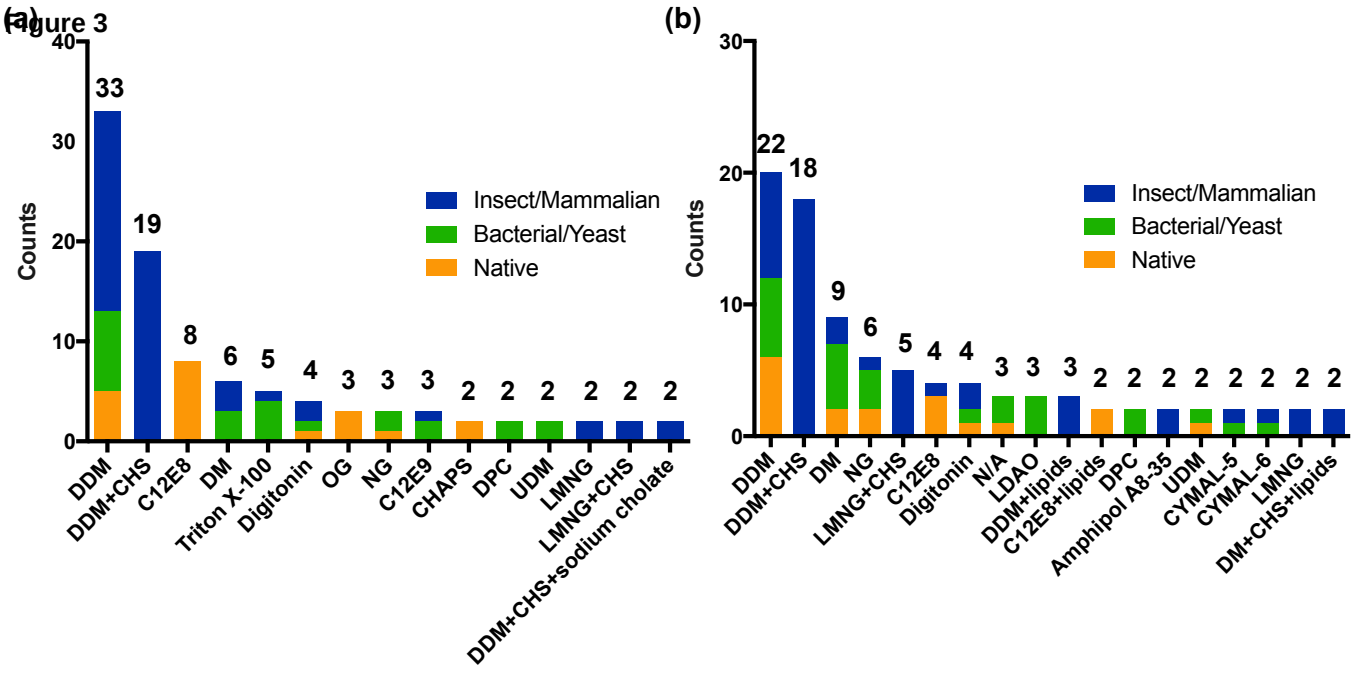
(a)
Counts
40
30
20
10
0
33
19
8
6
5
4
3
3
3
2
2
2
2
2
2
DDM
DDM+CHS
C12E8
DM
Triton X-100
Digitonin
OG
NG
C12E9
CHAPS
DPC
UDM
LMNG
LMNG+CHS
DDM+CHS+sodium cholate
Insect/Mammalian
Bacterial/Yeast
Native
(b)
Counts
30
20
10
0
22
18
9
6
5
4
4
3
3
3
2
2
2
2
2
2
2
DDM
DDM+CHS
DM
NG
LMNG+CHS
C12E8
Digitonin
N/A
LDAO
DDM+lipids
C12E8+lipids
DPC
Amphipol A8-35
UDM
CYMAL-5
CYMAL-6
LMNG
DM+CHS+lipids
Insect/Mammalian
Bacterial/Yeast
Native

Suppl. Figure 1

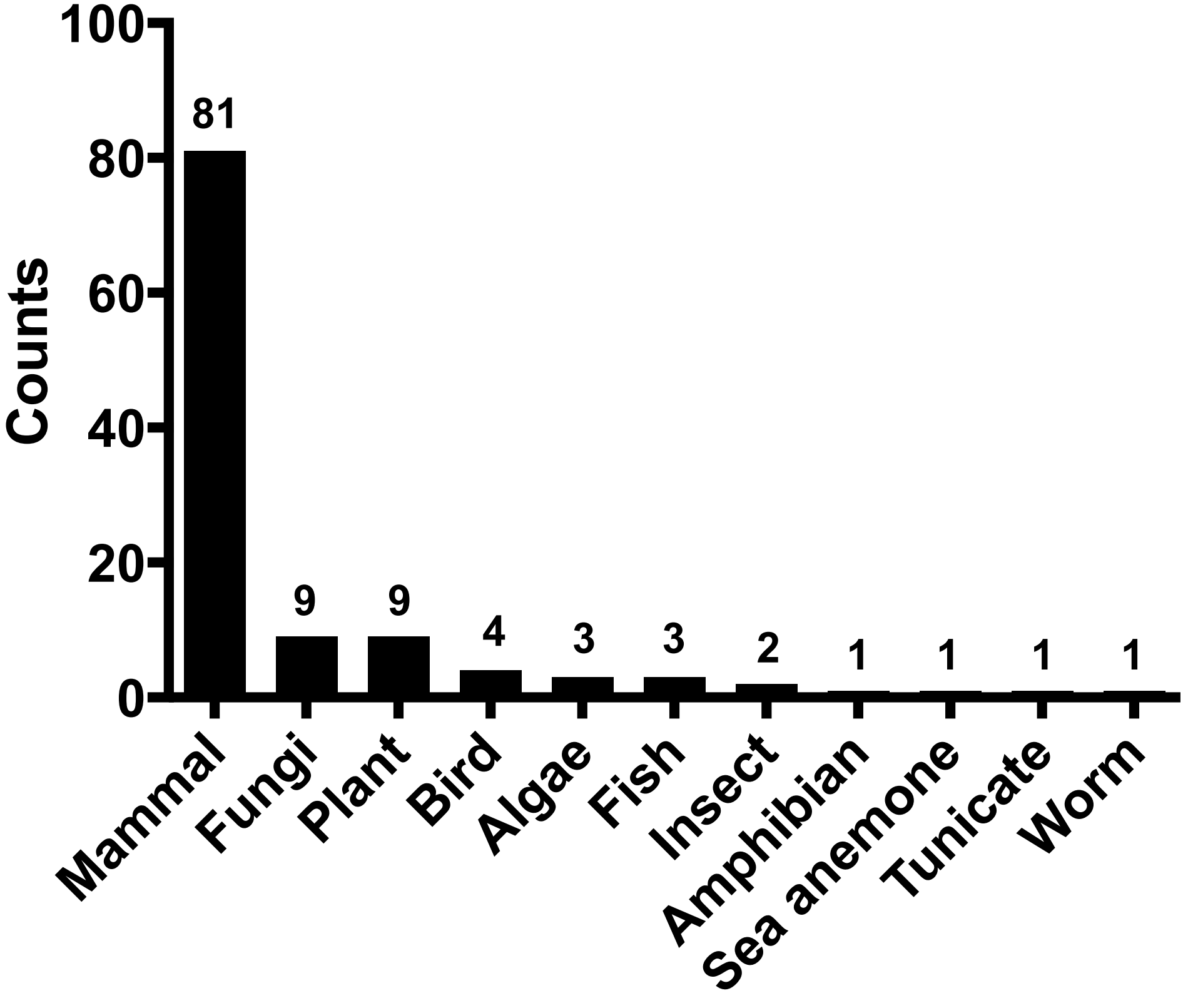

Suppl. Figure 2

(a)

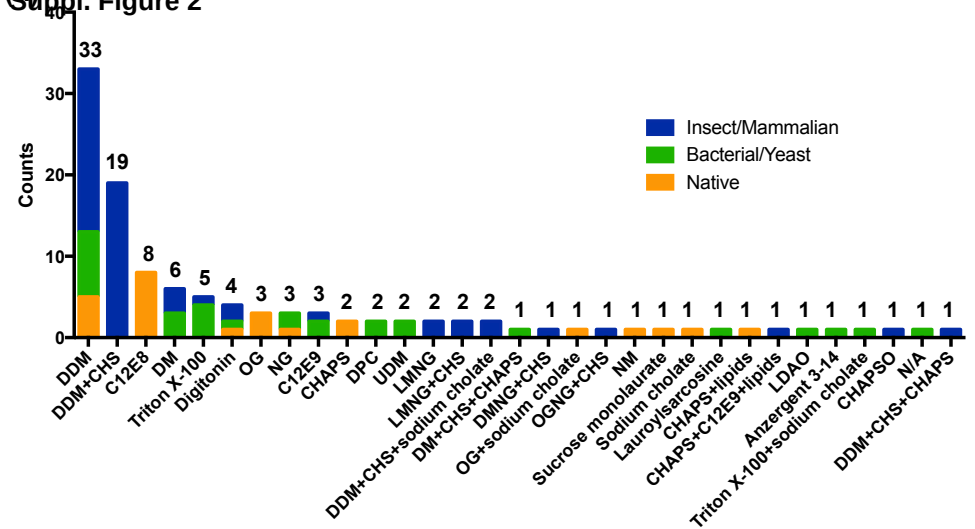

(b)

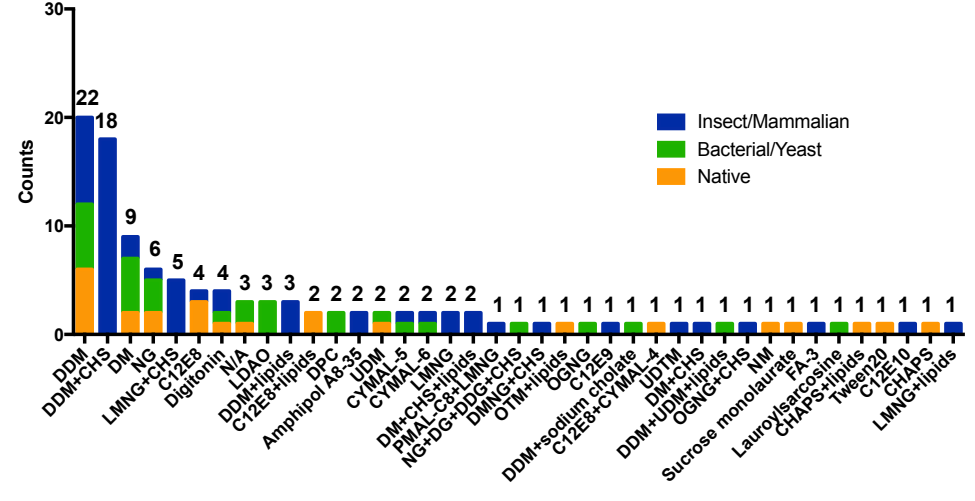

Suppl. Figure 3

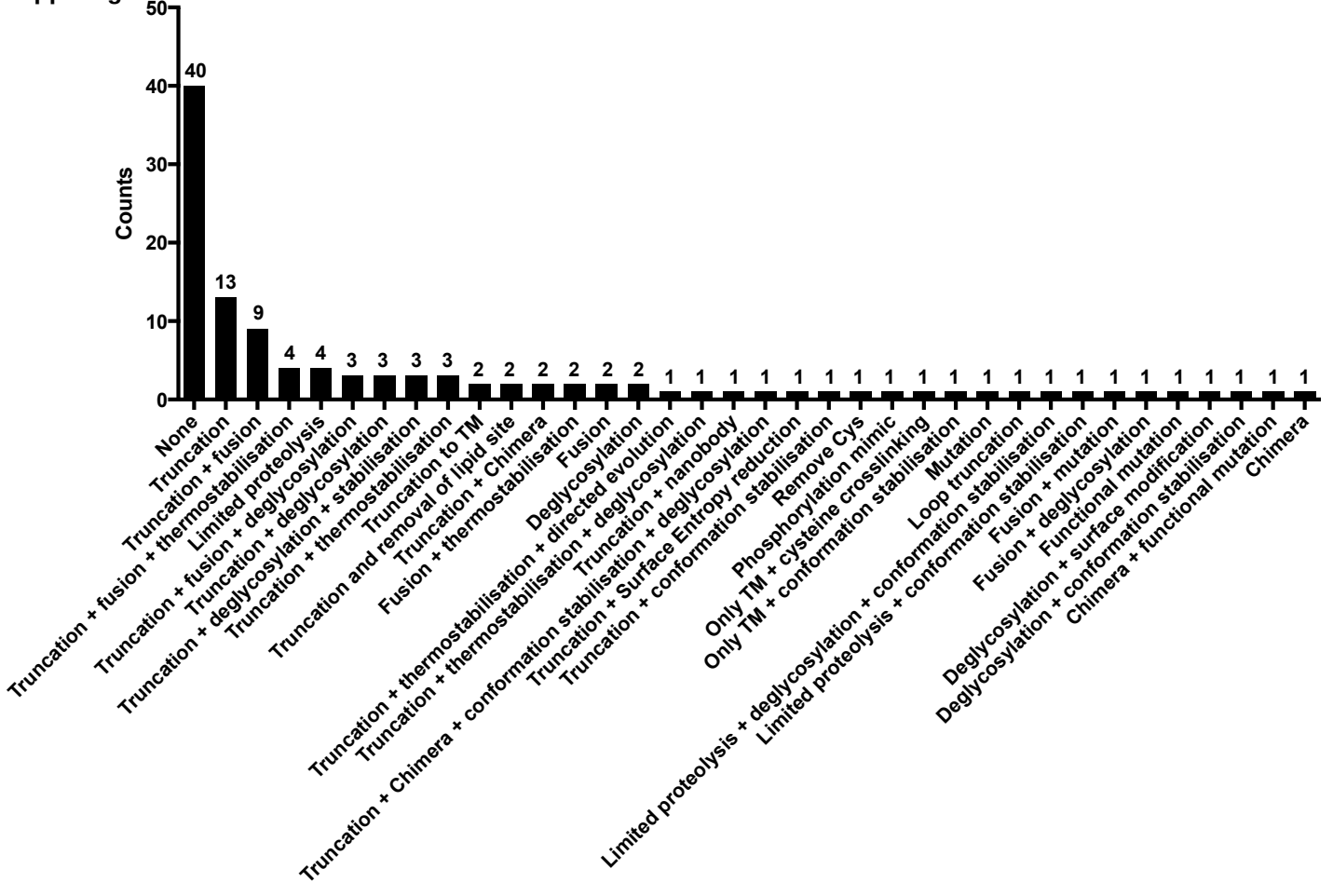

Supplementary Table 1

Supplementary Table 1: Eukaryotic integral membrane protein for whom structures have been released from 1st January 2014 to 8th March 2016

Protein name/ description*	Source/ Expression host§	Stabilisation strategy	Tags	Detergent#		Structural method	Reference/ PDB ID(s)
				Solubilisation	Purification		
G-Protein Coupled Receptors							
Free fatty-acid receptor 1 (GPR40) - T4L fusion	*H. sapiens/ S. frugiperda*	Thermostabilising mutations with T4L fusion	FLAG + His	DDM + CHS	LMNG + CHS	X-ray, LCP in monoolein	[1] 4PHU
Opsin in complex with the finger-loop peptide derived from arrestin-1	*B. taurus/ Native*	None	N/A	OG	Not reported	X-ray, Vapour Diffusion	[2] 4PXF
OX2 orexin receptor - PGS fusion bound to the insomnia drug Suvorexant	*H. sapiens/ S. frugiperda*	Termini truncation and fusion to P. abysii glycogen synthase (PGS)	FLAG	DDM + CHS + sodium cholate	LMNG	X-ray, LCP in monoolein	[3] 4S0V
Rhodopsin-Arrestin complex - T4L fusion	*H. sapiens/ H. sapiens*	Thermostabilising mutations and expressed as a T4L-rhodopsin-arrestin fusion	MBP	DDM + CHS	LMNG + CHS	X-ray, LCP in monoolein	[4] 4ZWJ
Mu-type opioid receptor bound to an agonist	*M. musculus/ S. frugiperda*	Truncation of termini and bound to a camelid nanobody	FLAG + His	DDM + CHS + CHAPS	LMNG + CHS	X-ray, LCP in monoolein	[5] 5C1M
Opioid delta receptor - BRIL fusion in complex with a bifunctional peptide	*H. sapiens/ S. frugiperda*	Termini truncation and addition of BRIL fusion to N-terminus	FLAG + His	DDM + CHS	DDM + CHS	X-ray, LCP in monoolein	[6] 4RWA, 4RWD
C-X-C chemokine receptor type 4 - T4L-SGS fusion	*H. sapiens/ S. frugiperda*	Truncation of C-terminus, thermostabilising mutations, replacement of ICL3 with a T4L-SGS fusion and cys-crosslinking to antagonist	FLAG + His	DDM + CHS	DDM + CHS	X-ray, LCP in monoolein and cholestrol	[7] 4RWS
Muscarinic acetylcholine receptor M3 - T4L Fusion bound to an antagonist	*R. norvegicus/ S. frugiperda*	Truncation of N- and C-terminus, deglycosylation mutations and replacement of ICL3 with a disulphide stabilised T4L fusion.	FLAG + His	DDM + CHS + sodium cholate	LMNG + CHS	X-ray, LCP in monoolein and cholestrol	[8] 4U14
Adenodine A2A receptor bound to an agonist	*H. sapiens/ T. ni*	Truncation of C-terminus, removal of glycosylation site and addition of thermostabilising mutations	10xHis	DM	DM + CHS	X-ray, LCP	[9] 4UG2, 4UHR

Protein name/ description*	Source/ Expression host[§]	Stabilisation strategy	Tags	Detergent[#]		Structural method	Reference/ PDB ID(s)
				Solubilisation	Purification		
Opsin in complex with a high-affinity peptide mimetic of the C terminus of transducin	*B. taurus/ Native*	None	N/A	NG	NG	X-ray,Vapour diffusion	[10] 4X1H
Neurotensin receptor type 1 - T4L fusion bound to neurotensin fragment	*R. norvegicus/ T. ni*	Truncation of N- and C-terminus, thermostabilising mutations and replacement of ICL3 with a T4L fusion	FLAG + His	LMNG + CHS	LMNG + CHS	X-ray, LCP in monoolein and cholestrol	[11] 4XEE, 4XES
P2Y purinoceptor 1 - Rubredoxin fusion in complex with a non-nucleotide antagonist	*H. sapiens/ S. frugiperda*	Replacement of ICL3 with rubredoxin and removal of glycosylation site	FLAG + His	DDM + CHS	DDM + CHS	X-ray, LCP in monoolein and cholestrol	[12] 4XNV
P2Y purinoceptor 1 - Rubredoxin/BRIL fusion in complex with a nucleotide antagonist	*H. sapiens/ S. frugiperda*	N-terminal truncation with addition of BRIL fusion, replacement of ICL3 with rubredoxin and removal of glycosylation site	FLAG + His	DDM + CHS	DDM + CHS	X-ray, LCP in monoolein and cholestrol	[12] 4XNW
Angiotensin Receptor - BRIL fusion bound to an antagonist	*H. sapiens/ S. frugiperda*	Truncation of N- and C-termini and addition of BRIL as an N-terminal fusion	FLAG + His	DDM + CHS	DDM + CHS	X-ray, LCP in monoolein and cholestrol	[13] 4YAY
Lysophosphatidic acid receptor 1 - BRIL fusion bound to various antagonists	*H. sapiens/ S. frugiperda*	Truncation of C-terminus and replacement of ICL3 with BRIL fusion	10xHis	DDM + CHS	DDM + CHS	X-ray, LCP in monoolein and cholestrol	[14] 4Z34, 4Z35, 4Z36
Type-1 angiotensin II receptor - BRIL fusion bound to an inverse agonist	*H. sapiens/ S. frugiperda*	Truncation of N- and C-termini and addition of BRIL as an N-terminal fusion	FLAG + His	DDM + CHS	DDM + CHS	X-ray, LCP in monoolein and cholestrol	[15] 4ZUD
Metabotropic glutamate receptor 5 (TM domain) (mGlu5) - T4L fusion in complex with negative allosteric modulators	*H. sapiens/ S. frugiperda*	Truncation of N- and C-termini, thermostabilising mutations and replacement of ICL2 with a T4L fusion	8xHis	DDM	DDM	X-ray, LCP in monoolein and cholestrol	[16] 5CGC, 5CGD
Beta-2 adrenergic receptor bound to a partial inverse agonist	*H. sapiens/ S. frugiperda*	Truncation of C-terminus, removal of glycosylation site and replacement of ICL3 with T4L fusion	FLAG	DDM + CHS	DDM + CHS	X-ray, LCP	[17] 5D5A, 5D5B

Protein name/ description*	Source/ Expression host[§]	Stabilisation strategy	Tags	Detergent[#]		Structural method	Reference/ PDB ID(s)
				Solubilisation	Purification		
NOP receptor (nociceptin/orphanin FQ peptide receptor (NOP)) - BRIL fusion with various antagonists	*H. sapiens/ S. frugiperda*	Truncation of N- and C-termini and addition of BRIL as an N-terminal fusion	FLAG + His	DDM + CHS	DDM + CHS	X-ray, LCP in monoolein and cholestrol	[18] 5DHG, 5DHH
Neurotensin receptor type 1 bound to agonists in thermostable or evolved forms	*R. norvegicus/ E. coli*	Directed evolution, CHESS, truncation of ICL3 and both termini	6xHis	DM + CHS + CHAPS	NG + DG + DDG + CHS	X-ray,Vapour diffusion	[19] 3ZEV, 4BUO, 4BV0, 4BWB
Smoothened receptor (SMO) - BRIL fusion in antagonist and agonist bound states	*H. sapiens/ S. frugiperda*	Truncation of N- and C-termini and addition of BRIL as an N-terminal fusion or replacing ICL3	FLAG + His	DDM + CHS	DDM + CHS	X-ray, LCP in monoolein	[20] 4N4W, 4QIM, 4QIN
P2Y purinoceptor 12 - BRIL fusion in complex with with a non-nucleotide reversible antagonist	*H. sapiens/ S. frugiperda*	Replacement of ICL3 with BRIL fusion and addition of yield improving mutation	10xHis	DDM + CHS	DDM + CHS	X-ray, LCP in monoolein	[21] 4NTJ
Metabotropic glutamate receptor 5 (TM domain) - T4L fusion in complex with a negative allosteric modulator	*H. sapiens/ S. frugiperda*	Truncation of N- and C-termini, thermostabilising mutations and replacement of ICL2 with a T4L fusion	8xHis	DDM	DDM	X-ray, LCP in monoolein	[22] 4OO9
Metabotropic glutamate receptor 1 (TM domain) - BRIL fusion in complex with a negative allosteric modulator	*H. sapiens/ S. frugiperda*	Truncation of N- and C-termini, and fusion of BRIL to N-terminus	FLAG + His	DDM + CHS	DDM + CHS	X-ray, LCP in monoolein	[23] 4OR2
P2Y purinoceptor 12 - BRIL fusion in complex with with nucleotide derived full and partial agonists	*H. sapiens/ S. frugiperda*	Replacement of ICL3 with BRIL fusion and addition of yield improving mutation	FLAG + His	DDM + CHS	DDM + CHS	X-ray, LCP in monoolein	[24] 4PXZ, 4PY0
Pentameric ligand-gated ion channels (pLGICs/Cys loop receptors)							
Gamma-aminobutyric acid receptor, (GABA(A)R-beta3 homopentamer)	*H. sapiens/ HEK293S-GnTI–*	Truncation of ICL2 and replacement by a 7 residue linker	1D4	DMNG + CHS	DMNG + CHS	X-ray,Vapour diffusion	[25] 4COF
Serotonin receptor (5-HT3-A homopentamer)	*M. musculus H. sapiens T-REx-*	Limited proteolysis with trypsin, deglycosylated with PNGaseF and	4xStrepII	C12E9	C12E9	X-ray,Vapour diffusion	[26] 4PIR

Protein name/ description*	Source/ Expression host[§]	Stabilisation strategy	Tags	Detergent[#]		Structural method	Reference/ PDB ID(s)
				Solubilisation	**Purification**		
	293	use of nanobodies					
Glycine Receptor (GlyR alpha-1 homopentamer) in strychnine-, glycine-, and glycine/ivermectin-bound states	*D. rerio/ S. frugiperda*	Removal of residues from both termini and replacement of ICL2 with a tripeptide	8xHis	DDM	DDM	EM	[27] 3JAD, 3JAE, 3JAF
Glycine Receptor (GlyR alpha-3 homopentamer) in a strychnine bound state	*H. sapiens/ S. frugiperda*	Truncation of C-terminus and replacement of ICL2 with a tripeptide	StrepII	DDM	DDM	X-ray, Vapour diffusion	[28] 5CFB
Glutamate-gated ion channels (GICs)							
AMPA receptor (GluA2 homotetramer) in resting, pre-open, and desensitized States	*R. norvegicus/ HEK293S GnTI−*	Five or ten thermostabilising mutations, and truncation of ICL1 and the ATD-LBD linker	8xHis	DDM	UDTM	X-ray,Vapour diffusion	[29] 4U1W, 4U2P, 4U2Q, 4U1X, 4U1Y
AMPA receptor (GluA2 homotetramer) in an antagonist bound state	*R. norvegicus/ S. frugiperda*	Truncation of C-terminus and addition of two mutation that improve expression and tetramer stabilisation	8xHis	DDM + CHS	DDM + CHS	Electron microscopy	[30] 4UQ6
AMPA receptor (GluA2 homotetramer) in antagonist and partial agonist bound states	*R. norvegicus/ S. frugiperda*	Truncations with deglycosylation and mutations to stabilize tetrameric state	8xHis	DDM	DDM + lipids	X-ray, Vapour diffusion	[31] 4U4F, 4U4G
AMPA receptor (GluA2 homotetramer) in a toxin, partial agonist and allosteric modulator bound state	*R. norvegicus/ H. sapiens*	Truncation of ICL1, ten thermostabilising mutations and removal of glycosylation site	8xHis	DDM	DDM + lipids	X-ray, Vapour diffusion	[32] 4U5B, 4U5C, 4U5D, 4U5E, 4U5F
NMDA receptor (GluN1/GluN2B heterodimer) bound to GluN2B specific allosteric modulator, GluN1 and GluN2B partial agonists and ion channel blocker	*X. laevis/ HEK293S GnTI−*	Replacement of C-terminus with 11 residues from GluA2, mutations to remove reactive cysteines and glycosylation sites, reduce surface entropy, and improve thermostability, conformational homogeneity and expression levels	C-terminal 8xHis (N1) or StrepII (N2B)	LMNG + CHS	DDM + CHS	X-ray, Vapour diffusion	[33] 4TLL, 4TLM

Protein name/ description*	Source/ Expression host[§]	Stabilisation strategy	Tags	Detergent[#]		Structural method	Reference/ PDB ID(s)
				Solubilisation	Purification		
NMDA receptor (GluN1/GluN2B heterodimer) bound to an allosteric inhibitor and GluN1 and GluN2B specific agonists	*R. norvegicus/ S. frugiperda*	Truncation of termini and ATD-LBD linker, mutations to remove glycosylation sites, engineer cysteine crosslinking and reduce surface entropy.	Onestrep	LMNG	LMNG + lipids	X-ray, Vapour diffusion	[34] 4PE5
Ligand-gated ion channels (LICs)							
Inositol 1,4,5-trisphosphate receptor type 1 (IP3 receptor type 1) in an apo state	*R. norvegicus/ Native*	None	Antibody	CHAPS	CHAPS	Electron microscopy	[35] 3JAV
Ryanodine receptor 1 (RyR1) in a calcium free, calbastin2 bound state	*O. cuniculus/ Native*	None	N/A	CHAPS	CHAPS + lipids	Electron microscopy	[36] 3J8E
Ryanodine receptor 1 (RyR1) in complex with FKBP12	*O. cuniculus/ Native*	None	N/A	CHAPS + lipids	Tween20	Electron microscopy	[37] 3J8H
Calcium-activated chloride channels							
Bestrophin-1	*G. gallus/ P. pastoris*	Truncation of C-terminus	Anti-tubulin tag	DDM	CYMAL-6	X-ray,Vapour diffusion with antibody	[38] 4RDQ
Voltage-dependent calcium channel (VDCCs)							
L-type voltage-gated calcium channel Cav1.1	*O. cuniculus/ Native*	None	N/A	Digitonin	Digitonin	Electron microscopy	[39] 3JBR
Transient receptor potential (TRP) channels							
Transient receptor potential cation channel subfamily V member 1 (capsaicin receptor, TRPV1)	*R. norvegicus/ HEK293S GnTI−*	Truncation of termini and removal of a divergent sequence region 604-626	MBP	DDM	Amphipol A8-35	Electron microscopy	[40] 3J9J

Protein name/ description*	Source/ Expression host[§]	Stabilisation strategy	Tags	Detergent[#]		Structural method	Reference/ PDB ID(s)
				Solubilisation	Purification		
Transient receptor potential cation channel subfamily A member 1 (TRPA1)	*H. sapiens/ HEK293S GnTI−*	MBP fusion	MBP	LMNG	PMAL-C8 + LMNG	Electron microscopy	[41] 3J9P
Voltage-dependent anion channels (VDACs)							
Voltage dependent anion channel 2 (VDAC2)	*D. rerio/ E. coli*	None	6xHis	Triton X-100	LDAO	X-ray,Vapour diffusion	[42] 4BUM
Voltage dependent anion channel 1 (VDAC1)	*M. musculus/ E. coli*	None	6xHis	LDAO	LDAO	X-ray, Bicelles	[43] 4C69
Voltage-gated proton channels							
Voltage-gated proton channel (Hv)	*M. musculus/ S. frugiperda*	Truncation of N-terminus and a chimera replacing the cytoplasmic coiled coil and the cytoplasmic halves of S2 and S3 with the leucine-zipper transcriptional activator GCN4 from S. cerevisiae and the intracellular portion of C. intestinalis voltage sensing phosphatase, respectively	8xHis	DDM	CYMAL-5	X-ray,Vapour diffusion	[44] 3WKV
Voltage gated sodium channels							
Chimera of NavAB with voltage sensor domain 4 of Nav1.7	*H. sapiens/ T. ni*	Chimera of VSD4 of Nav1.7 with the bacterial NavAb channel	FLAG	Digitonin	Digitonin	X-ray, Bicelles	[45] 5EK0
Acid sensing ion channel/epithelial sodium channel/degenerin (ASIC/ENaC/DEG family)							
Acid-sensing ion channel 1a (in complex with snake toxin, amiloride, and cesium)	*G. gallus/ HEK 293 GnTI−*	Truncation of N- and C-termini	8xHis	DDM	DDM	X-ray,Vapour diffusion	[46] 4NTW, 4NTX, 4NTY
Acid-sensing ion channel 1a in a desensitized state	*G. gallus/ S. frugiperda*	Truncation of C-terminus	8xHis	DDM	DDM	X-ray,Vapour diffusion	[47] 4NYK

Protein name/ description*	Source/ Expression host[§]	Stabilisation strategy	Tags	Detergent[#]		Structural method	Reference/ PDB ID(s)
				Solubilisation	Purification		
2-pore domain K+ (K2P) channels							
TWIK-related K+ channel 2 (TREK2) - In apo forms and in complexes with norfluoxetine and Br-fluoxetine.	*H. sapiens/ S. frugiperda*	Truncation of N- and C- termini	FLAG + His	OGNG + CHS	OGNG + CHS	X-ray,Vapour diffusion	[48] 4BW5, 4XDJ, 4XDK, 4XDL
TWIK-related arachidonic acid-stimulated K+ channel (TRAAK) - Tl+ and K+ bound in conductive and nonconductive states	*H. sapiens/ P. pastoris*	Truncation of N- and C- termini and removal of glycosylation sites	10xHis	DM	DM	X-ray, Vapour Diffusion with antibody	[49] 4WFE, 4WFF, 4WFG, 4WFH
Slo family of large conductance K+ channel							
Slo2.2 sodium activated potassium channel - in a sodium free state	*G. gallus/ S. frugiperda*	None	FLAG	DDM	DDM + lipids	Electron microscopy	[50] 5A6E, 5A6G
The Mechanical Nociceptor, Piezo (Piezo) Family							
Piezo-type mechanosensitive ion channel 1 (Piezo 1)	*M. musculus/ H. sapiens*	None	GST	CHAPS + C12E9 + lipids	C12E10	Electron microscopy	[51] 3JAC
Claudins							
Claudin-15	*M. musculus/ S. frugiperda*	Truncation of C-terminus and removal of palmitoylation sites	8xHis	DDM	LMNG	X-ray, LCP with monoolein	[52] 4P79
Claudin-19 bound to a C-terminal fragment of an enterotoxin	*M. musculus/ S. frugiperda*	Truncation of C-terminus and removal of palmitoylation sites	8xHis	DDM + CHS	DDM	X-ray,Vapour diffusion	[53] 3X29
Neurotransmitter: sodium symporters (NSSs)							
Dopamine transporter in complexes with nisoxetine and reboxetine	*D. melanogaster/ HEK-293S GnTI−*	Truncation of ECL2, N- and C-termini truncation, with various thermostabilising mutations	8xHis	DDM	DM + CHS + lipids	X-ray, Vapour Diffusion with Fab Ab	[54] 4XNU, 4XNX

Protein name/ description*	Source/ Expression host[§]	Stabilisation strategy	Tags	Detergent[#]		Structural method	Reference/ PDB ID(s)
				Solubilisation	**Purification**		
Dopamine transporter in complex with different ligands (dopamine, a substrate analogue 3,4-dichlorophenethylamine, the psychostimulants D-amphetamine and methamphetamine, or to cocaine and cocaine analogues)	*D. melanogaster/ HEK-293S GnTI–*	Truncation of ECL2, N- and C-termini truncation, with various thermostabilising mutations	8xHis	DM + CHS	DM + CHS + lipids	X-ray, Vapour Diffusion with Fab 9D5 antibody	[55] 4XP1, 4XP4, 4XP5, 4XP6, 4XP9, 4XPA, 4XPB, 4XPF, 4XPG, 4XPH, 4XPT
ATP-binding cassette transporters (ABC transporters)							
Mitochondrial ABC transporter Atm1 - with and without glutathione bound	*S. cerevisiae/ E. coli*	Truncation of N-terminus	StrepII	DDM	DDM	X-ray,Vapour diffusion	[56] 4MYC, 4MYH
CmABCB1 (P-gp homolog) - in an apo state	*C. merolae/ P. pastoris*	Limited proteolysis with trypsin to remove N-terminus	His	C12E9	DM	X-ray, Vapour diffusion	[57] 3WME
CmABCB1 (P-gp homolog) - in an apo and cyclic peptide bound state	*C. merolae/ S. cerevisiae*	Limited proteolysis with trypsin to remove N-terminus and triple mutant to reduce flexibility	FLAG + His	C12E9	DM	X-ray, Vapour diffusion	[57] 3WMG, 3WMF
P-glycoprotein (P-gp) - in complex with various ligands	*M. musculus/ P. pastoris*	Removal of deglycosylation sites and surface modification with reductive amination	6xHis	Triton X-100	DDM + sodium cholate	X-ray,Vapour diffusion	[58] 4Q9H, 4Q9I, 4Q9J, 4Q9K, 4Q9L
P-type ATPase							
Sarcoplasmic reticulum calcium ATPase (SERCA1a) in calcium bound state	*O. cuniculus/ Native*	None	N/A	C12E8	C12E8 and PC	Electron crystallography , Dialysis	[59] 3J7T
Sarcoplasmic reticulum calcium ATPase (SERCA1a) E2(TG) in the presence of added lipids	*O. cuniculus/ Native*	None	N/A	C12E8	C12E8 and PC	X-ray, HiLiDE	[60] 4UU0, 4UU1
Sarcoplasmic reticulum calcium ATPase (SERCA1a) phosphlamban bound	*O. cuniculus/ Native*	None	N/A	unknown	unknown	X-ray, HiLiDE	[61] 4Y3U

Protein name/ description*	Source/ Expression host[§]	Stabilisation strategy	Tags	Detergent[#]		Structural method	Reference/ PDB ID(s)
				Solubilisation	Purification		
Sarcoplasmic reticulum calcium ATPase (SERCA1a) in a calcium free, cyclopiazonic acid bound state	*O. cuniculus/ Native*	None	N/A	C12E8	C12E8	X-ray, Dialysis	[62] 4YCL
Sarcoplasmic reticulum calcium ATPase (SERCA1a) bound to marine macrolide inhibitors	*O. cuniculus/ Native*	None	N/A	C12E8	C12E8	X-ray, Dialysis	[63] 4YCM, 4YCN
Sarcoplasmic reticulum calcium ATPase (SERCA1a) in the Ca2-E1-MgAMPPCP state	*O. cuniculus/ Native*	None	N/A	C12E8	N/A	X-ray, Batch	[64] 4XOU
Na, K-ATPase (in complex with digoxin and bufalin)	*S. scrofa/ Native*	None	N/A	C12E8	C12E8 + CYMAL-4	X-ray, Vapour Diffusion with HiLiDe	[65] 4RES, 4RET
Na, K-ATPase in the E2·MgF42−·2K+ state in the presence of thallium or rubidium at various incubation times	*S. acanthias/ Native*	None	N/A	C12E8	C12E8	X-ray, Dialysis	[66] 5AVQ, 5AVR, 5AVS, 5AVT, 5AVU, 5AVV, 5AVW, 5AVX, 5AVY, 5AVZ, 5AW1, 5AW2, 5AW3, 5AW4, 5AW5, 5AW6, 5AW7, 5AW8, 5AW9, 5AW0
F-type ATPase (ATP synthase)							
CF1FO-ATP synthase - *c*14 ring	*T. aestivum/ Native*	None	N/A	OG + sodium cholate	DDM	X-ray,Vapour diffusion	[67] 4MJN
F1FO-ATP synthase - *c*10 ring bound to oligomycin	*S. cerevisiae/ S. cerevisiae*	None	6xHis	DDM	DDM	X-ray, bicelles	[68] 4F4S, 5BPS, 5BQ6, 5BQA, 5BQJ

Protein name/ description*	Source/ Expression host[§]	Stabilisation strategy	Tags	Detergent[#]		Structural method	Reference/ PDB ID(s)
				Solubilisation	Purification		
V-type ATPase							
Vacuolar H+-ATPases (V-ATPases) in various rotational states	*S. cerevisiae/ S. cerevisiae*	None	FLAG	DDM	DDM	Electron microscopy	[69] 3J9T, 3J9U, 3J9V
Glucose transporter (Solute carrier family 2)							
Glucose transporter (GLUT1) in an inward-open conformation	*H. sapiens/ T. ni*	Removal of a glycosylation site and conformation stabilising mutation	10xHis	DDM	NG	X-ray,Vapour diffusion	[70] 4PYP
Glucose transporter 3 (GLUT3) in glucose and maltose bound forms	*H. sapiens/ S. frugiperda*	Removal of a glycosylation site	10xHis	DDM	CYMAL-6	X-ray, LCP in monoolein	[71] 4ZW9, 4ZWB, 4ZWC
Glucose transporter 3 (GLUT3)	*H. sapiens/ S. frugiperda*	Truncation of C-terminus and removal of glycosylation site	Not reported	Not reported	Not reported	X-ray, not reported	5C65
Glucose transporter 5 (GLUT5) in an open inward-facing conformation	*R. norvegicus/ S. cerevisiae*	Removal of a glycosylation site	8xHis	DDM	DDM	X-ray, Vapour diffusion with antibody	[72] 4YBQ
Glucose transporter 5 (GLUT5) in an open inward-facing conformation	*B. taurus/ S. cerevisiae*	Truncation of C-terminus and removal of glycosylation site	8xHis	DDM	UDM	X-ray, Vapour diffusion	[72] 4YB9
SWEET							
Bidirectional sugar transporter SWEET2b in an inward open conformation	*O. sativa/ P. pastoris*	Truncation of C-terminus	His	DDM	NG	X-ray, Vapour diffusion	[73] 5CTG, 5CTH
PTR family							
Nitrate transporter 1.1	*A. thaliana/ T. ni*	None	8xHis	DDM	DDM	X-ray,Vapour diffusion	[74] 4OH3
Nitrate transporter 1.1	*A. thaliana/ S. cerevisiae*	None	His	DDM	DDM	X-ray, Vapour diffusion	[75] 5A2N, 5A2O

Protein name/ description*	Source/ Expression host[§]	Stabilisation strategy	Tags	Detergent[#]		Structural method	Reference/ PDB ID(s)
				Solubilisation	Purification		
TMEM16 family (anoctamins)							
TMEM16 lipid scramblase (in 2 different crystal forms)	*N. haematococca/ S. cerevisiae*	None	10xHis	DDM	DDM + UDM + lipids	X-ray,Vapour diffusion	[76] 4WIS, 4WIT
Water Channels							
Aquaporin-2	*H. sapiens/ P. pastoris*	Truncation of C-terminus	8xHis	NG	OGNG	X-ray,Vapour diffusion	[77] 4NEF
Aquaporin-5	*H. sapiens/ P. pastoris*	Mutations to mimic phosphorylation	N/A	NG	NG	X-ray, Vapour diffusion	[78] 5C5X, 5DYE
Actinoporins							
Fragaceatoxin C	*A. fragacea/ E. coli*	None	N/A	Triton X-100	DDM	X-ray, Sponge phase	[79] 4TSY
Tryptophan-rich sensory proteins							
Translocator protein (TSPO)	*M. musculus/ E. coli*	None	N/A	DPC	DPC	Solution NMR	[80] 2MGY
Translocator protein (TSPO)	*M. musculus/ E. coli*	None	N/A	DPC	DPC	Solution NMR	[81] 2N02
Complex I							
NADH Ubiquinone oxidoreductase	*B. taurus/ Native*	None	N/A	DDM	DDM	Electron microscopy	[82] 4UQ8
Oxidoreductases							
Complex III (cytochrome bc1 complex, coenzyme Q-cytochrome c reductase) bound to the 4(1H)-pyridone class inhibitors.	*B. taurus/ Native*	None	N/A	DDM	DDM	X-ray,Vapour diffusion	[83] 4D6U, 4D6T
Complex III (cytochrome bc1 complex, coenzyme Q-cytochrome c reductase) bound to atovaquone	*S. cerevisiae/ Native*	None	N/A	DDM	UDM	X-ray, Vapour diffusion with antibody	[84] 4PD4

Protein name/ description*	Source/ Expression host[§]	Stabilisation strategy	Tags	Detergent[#]		Structural method	Reference/ PDB ID(s)
				Solubilisation	Purification		
Heme copper oxidase							
Cytochrome c oxidase	*B. taurus/ Native*	None	N/A	Not reported	DM	X-ray,Vapour diffusion	[85] 3WG7, 3X2Q
Ascorbate-dependent oxidoreductase enzymes							
Ascorbate-dependent oxidoreductase (Cytochrome b651) in apo and ascorbate bound states	*A. thaliana/ E. coli*	None	6xHis	DM	NG	X-ray,Vapour diffusion	[86] 4O6Y,4O79, 4O7G
Complex II							
Rhodoquinol-fumarate reductase bound to various inhibitors	*A. suum/ Native*	None	N/A	Sucrose monolaurate	Sucrose monolaurate	X-ray, Microdialysis	[87] 4YSX, 4YSY, 4YSZ, 4YT0, 4YTM, 4YTN, 5C2T
Succinate dehydrogenase bound to various inhibitors	*S. scrofa/ Native*	None	N/A	Sodium cholate	DDM	X-ray, Vapour diffusion	[87] 4YTP, 4YXD
Water-plastoquinone oxidoreductase							
Photoprotective protein PsbS in apo and DCCD inhibited state	*S. oleracea/ Native*	Limited proteolysis with subtilisin	N/A	OG	NG	X-ray,Vapour diffusion	[88] 4RI2, 4RI3
Photosynthetic reaction centre							
Photosystem I (PSI, plastocyanin: ferredoxin oxidoreductase)	*P. sativum/ Native*	None	N/A	Not reported	Not reported	Not reported	4RKU
Light Harvesting Complex II	*S. oleracea/ Native*	Limited proteolysis with trypsin to remove the N-terminus	N/A	OG	OTM + lipids	X-ray,Vapour diffusion	[89] 4LCZ
Photosystem I - light harvesting complex I supercomplex (PSI-LHCI)	*P. sativum/ Native*	None	N/A	DDM	DDM	X-ray, Batch method under oil	[90] 4XK8

Protein name/ description*	Source/ Expression host[§]	Stabilisation strategy	Tags	Detergent[#]		Structural method	Reference/ PDB ID(s)
				Solubilisation	Purification		
Progestin and adipoQ receptor family							
Adiponectin receptor 1	*H. sapiens/ T. ni*	Truncation of N-terminus	FLAG	DDM	DDM + CHS	X-ray, LCP with Fv of monoclonal antibody	[91] 3WXV
Adiponectin receptor 2	*H. sapiens/ T. ni*	Truncation of N-terminus	FLAG	DDM	DDM + CHS	X-ray, LCP with Fv of monoclonal antibody	[91] 3WXW
CYP51 cytochrome P450							
Lanosterol 14-alpha demethylase in complex with fluconazole, lanosterol, and itraconazole	*S. cerevisiae/ S. cerevisiae*	None	6xHis	DM	DM	X-ray,Vapour diffusion	[92] 4LXJ, 4WMZ, 5EQB
Connexin - gap junction protein							
Connexin-26 (Gap junction beta-2 protein) in calcium bound and free states	*H. sapiens/ S. frugiperda*	Mutation to prevent non native disulphide formation	6xHis	DM	FA-3	X-ray, Vapour diffusion	[93] 5ER7, 5ERA
ADP/ATP antiporter							
ADP/ATP carrier isoform 2	*S. cerevisiae/ S. cerevisiae*	None	8xHis	UDM	CYMAL-5	X-ray, Vapour diffusion	[94] 4C9G, 4C9H
ADP/ATP carrier isoform 2	*S. cerevisiae/ S. cerevisiae*	None	8xHis	UDM	DM	X-ray, Vapour diffusion	[94] 4C9J, 4C9Q
Fatty acid desaturases							
Stearoyl-CoA desaturase 1 (SCD1) in complex with substrate	*M. musculus/ T. ni*	Truncation of the N-terminus	His	DM	DM	X-ray, LCP in monoolein	[95] 4YMK
Stearoyl-CoA desaturase 1 (SCD1) in complex with substrate	*H. sapiens/ S. frugiperda*	Truncation of the N-terminus with mutations to improve the surface properties	6xHis	DDM	C12E8	X-ray, Vapour diffusion	[96] 4ZYO

Protein name/ description*	Source/ Expression host[§]	Stabilisation strategy	Tags	Detergent[#]		Structural method	Reference/ PDB ID(s)
				Solubilisation	Purification		
Membrane-Associated Proteins in Eicosanoid and Glutathione metabolism family (MAPEG)							
Leukotriene C4 synthase	*H. sapiens/ P. pastoris*	Mutations for binding studies	6xHis	Triton X-100 + sodium cholate	DDM	X-ray, Vapour diffusion	[97] 4J7T, 4J7Y, 4JC7, 4JRZ
Prostaglandin E2 synthase	*H. sapiens/ S. frugiperda*	Truncation of N-terminus and chimera with the C-terminus of LTC4S to generate crystal contact	FLAG + His	Triton X-100	DM	X-ray, LCP in monoolein	[98] 4BPM
Anion exchanger family							
Anion exchanger 1 - anion exchanger domain of Band 3 protein	*H. sapiens/ Native*	Limited proteolysis with trypsin to remove 40 kDa N-terminus	N/A	C12E8	DM	X-ray, Vapour diffusion with antibody	[99] 4YZF
Peptidases							
Gamma-secretase complex	*H. sapiens/ H. sapiens*	Fusion with T4L	FLAG	CHAPSO	Digitonin	Electron microscopy	[100] 4UIS
Gamma-secretase complex	*H. sapiens/ H. sapiens*	None	FLAG + His	Digitonin	Amphipol A8-35	Electron microscopy	[101] 5A63
Sialoglycoproteins							
Glycophorin-A transmembrane segment	*H. sapiens/ E. coli*	Truncation to TM domain	His	Triton X-100	N/A	X-ray, LCP in monoolein	[102] 5EH4, 5EH6
Epidermal growth factor receptor							
Receptor tyrosine-protein kinase erbB-2 (human epidermal growth factor receptor 2 (HER2))	*H. sapiens/ E. coli - Cell Free*	Truncation to TM and cytoplasmic juxtamembrane region A	N/A	Lauroyl-sarcosine	Lauroyl-sarcosine	Solution NMR	[103] 2N2A
Voltage sensitive phosphatases							
Voltage sensing domain of voltage sensor containing phosphase	*C. intestinalis/ E. coli*	Truncation to only the TM domain with a conformation stabilising mutation	His	Anzergent 3-14	LDAO	X-ray, Vapour diffusion	[104] 4G7Y, 4G80, 4G7V

Protein name/ description*	Source/ Expression host[§]	Stabilisation strategy	Tags	Detergent[#]		Structural method	Reference/ PDB ID(s)
				Solubilisation	Purification		
Archael Rhodopsins							
Sensory opsin A, Archaeal-type opsin 2 chimera	*C. reinhardtii/ S. frugiperda*	Functional mutations and chimerization with archael-type opsin 2	8xHis	DDM + CHS	DDM + CHS	X-ray, LCP with monoolein and cholesterol	[105] 4YZI
Protein translocase							
80S ribosome-Sec61 complex	*Y. lipolytica Native*	None	N/A	Digitonin	Digitonin	X-ray, Vapour diffusion	[106] 3J7R
TYRO protein tyrosine kinase-binding protein							
TYROBP - TM segment	*H. sapiens/ E. coli*	Truncation to TM domain and disulfide crosslinked homodimer	N/A	N/A	N/A	X-ray, LCP	[107] 4WO1, 4WOL

* Table comprises of entries released from the Protein Data Bank from 1st Jan 2014 to the 8th March 2016. In the case of multiple structures in a given citation - unique entries are defined based on unique source, expression host and construct design).

§ *Homo sapiens (H. sapiens), Bos taurus (b. taurus), Rattus norvegicus (R. rattus), Mus musculus (M. musculus), Danio rerio (D. rerio), Xenopus laevis (X. laevis), Oryctolagus cuniculus (O. cuniculus), Gallus gallus (G. gallus), Drosophila melanogaster (D. melanogaster), Saccharomyces cerevisiae (S. cerevisiae), Cyanidioschyzon merolae (C. merolae), Sus scrofa (S. scrofa), Squalus acanthias (S. acanthias), Triticum aestivum (T. aestivum), Oryza sativa (O. sativa), Nectria haematococca (N. haematococca), Actinia fragacea (A. fragacea), Ascaris suum (A. suum), Arabidopsis thaliana (A. thaliana), Spinacia oleracea (S. oleracea), Pisum sativum (P. sativum), Chlamydomonas reinhardtii (C. reinhardtii), Ciona intestinalis (C. intestinalis), Yarrowia lipolytica (Y. lipolytica), Pichia pastoris (P. pastoris), Escherichia coli (E. coli), Spodoptera frugiperda (S. frugiperda), Trichoplusia ni (T. ni).*

Dodecyl-β-D-maltoside (DDM), cholesteryl hemisuccinate (CHS), octaethylene glycol monododecyl ether (C12E8), decyl-β-D-maltoside (DM), octyl-β-D-glucoside (OG), nonaethylene glycol monododecyl ether (C12E9), 3-[(3-cholamidopropyl)dimethylammonio]-1-propanesulfonate (CHAPS), dodecylphosphocholine (DPC), undecyl-β-D-maltoside (UDM), lauryl maltose neopentyl glycol (LMNG), decyl maltose neopentyl glycol (DMNG), octyl glucose neopentyl glycol (OGNG), nonyl-β-D-maltoside (NM), lauryl dimethylamine N-oxide (LDAO), 3-[(3-cholamidopropyl)dimethylammonio]-2-hydroxy-1-propanesulfonate (CHAPSO), nonyl-β-D-glucoside (NG), 5-cyclohexyl-1-pentyl-β-D-maltoside (cymal-5), 6-cyclohexyl-1-hexyl-β-D-maltoside (cymal-6), Poly (maleic anhydride-alt-1-decene) substituted with 3-(dimethylamino) propylamine (PMAL-C8), dodecyl-β-D-glucopyranoside (DDG), octyl-β-D-thiomaltoside (OTM), 4-cyclohexyl-1-butyl-β-D-maltoside (cymal-4), undecyl-β-D-thiomaltoside (UDTM), 3α-hydroxy-7α,12α-di-((O-β-D-maltosyl)-2-hydroxyethoxy)-cholane (FA-3), decaethylene glycol monododecyl ether (C12E10).

References

1. Srivastava, A., J. Yano, Y. Hirozane, G. Kefala, F. Gruswitz, G. Snell, W. Lane, A. Ivetac, K. Aertgeerts, J. Nguyen, A. Jennings, and K. Okada, *High-resolution structure of the human GPR40 receptor bound to allosteric agonist TAK-875*. Nature, 2014. **513**(7516): p. 124-127.
2. Szczepek, M., F. Beyrière, K.P. Hofmann, M. Elgeti, R. Kazmin, A. Rose, F.J. Bartl, D. von Stetten, M. Heck, M.E. Sommer, P.W. Hildebrand, and P. Scheerer, *Crystal structure of a common GPCR-binding interface for G protein and arrestin*. Nat Commun, 2014. **5**.
3. Yin, J., J.C. Mobarec, P. Kolb, and D.M. Rosenbaum, *Crystal structure of the human OX2 orexin receptor bound to the insomnia drug suvorexant*. Nature, 2015. **519**(7542): p. 247-250.
4. Kang, Y., X.E. Zhou, X. Gao, Y. He, W. Liu, A. Ishchenko, A. Barty, T.A. White, O. Yefanov, G.W. Han, Q. Xu, P.W. de Waal, J. Ke, M.H.E. Tan, C. Zhang, A. Moeller, G.M. West, B.D. Pascal, N. Van Eps, L.N. Caro, S.A. Vishnivetskiy, R.J. Lee, K.M. Suino-Powell, X. Gu, K. Pal, J. Ma, X. Zhi, S. Boutet, G.J. Williams, M. Messerschmidt, C. Gati, N.A. Zatsepin, D. Wang, D. James, S. Basu, S. Roy-Chowdhury, C.E. Conrad, J. Coe, H. Liu, S. Lisova, C. Kupitz, I. Grotjohann, R. Fromme, Y. Jiang, M. Tan, H. Yang, J. Li, M. Wang, Z. Zheng, D. Li, N. Howe, Y. Zhao, J. Standfuss, K. Diederichs, Y. Dong, C.S. Potter, B. Carragher, M. Caffrey, H. Jiang, H.N. Chapman, J.C.H. Spence, P. Fromme, U. Weierstall, O.P. Ernst, V. Katritch, V.V. Gurevich, P.R. Griffin, W.L. Hubbell, R.C. Stevens, V. Cherezov, K. Melcher, and H.E. Xu, *Crystal structure of rhodopsin bound to arrestin by femtosecond X-ray laser*. Nature, 2015. **523**(7562): p. 561-567.
5. Huang, W., A. Manglik, A.J. Venkatakrishnan, T. Laeremans, E.N. Feinberg, A.L. Sanborn, H.E. Kato, K.E. Livingston, T.S. Thorsen, R.C. Kling, S. Granier, P. Gmeiner, S.M. Husbands, J.R. Traynor, W.I. Weis, J. Steyaert, R.O. Dror, and B.K. Kobilka, *Structural insights into [micro]-opioid receptor activation*. Nature, 2015. **524**(7565): p. 315-321.
6. Fenalti, G., N.A. Zatsepin, C. Betti, P. Giguere, G.W. Han, A. Ishchenko, W. Liu, K. Guillemyn, H. Zhang, D. James, D. Wang, U. Weierstall, J.C.H. Spence, S. Boutet, M. Messerschmidt, G.J. Williams, C. Gati, O.M. Yefanov, T.A. White, D. Oberthuer, M. Metz, C.H. Yoon, A. Barty, H.N. Chapman, S. Basu, J. Coe, C.E. Conrad, R. Fromme, P. Fromme, D. Tourwé, P.W. Schiller, B.L. Roth, S. Ballet, V. Katritch, R.C. Stevens, and V. Cherezov, *Structural basis for bifunctional peptide recognition at human δ-opioid receptor*. Nat Struct Mol Biol, 2015. **22**(3): p. 265-268.
7. Qin, L., I. Kufareva, L.G. Holden, C. Wang, Y. Zheng, C. Zhao, G. Fenalti, H. Wu, G.W. Han, V. Cherezov, R. Abagyan, R.C. Stevens, and T.M. Handel, *Crystal structure of the chemokine receptor CXCR4 in complex with a viral chemokine*. Science, 2015. **347**(6226): p. 1117-1122.
8. Thorsen, Thor S., R. Matt, William I. Weis, and Brian K. Kobilka, *Modified T4 Lysozyme Fusion Proteins Facilitate G Protein-Coupled Receptor Crystallogenesis*. Structure, 2014. **22**(11): p. 1657-1664.
9. Lebon, G., P.C. Edwards, A.G.W. Leslie, and C.G. Tate, *Molecular Determinants of CGS21680 Binding to the Human Adenosine A2A Receptor*. Molecular Pharmacology, 2015. **87**(6): p. 907-915.
10. Blankenship, E., A. Vahedi-Faridi, and David T. Lodowski, *The High-Resolution Structure of Activated Opsin Reveals a Conserved Solvent Network in the Transmembrane Region Essential for Activation*. Structure, 2015. **23**(12): p. 2358-2364.
11. Krumm, B.E., J.F. White, P. Shah, and R. Grisshammer, *Structural prerequisites for G-protein activation by the neurotensin receptor*. Nat Commun, 2015. **6**.

12. Zhang, D., Z.-G. Gao, K. Zhang, E. Kiselev, S. Crane, J. Wang, S. Paoletta, C. Yi, L. Ma, W. Zhang, G.W. Han, H. Liu, V. Cherezov, V. Katritch, H. Jiang, R.C. Stevens, K.A. Jacobson, Q. Zhao, and B. Wu, *Two disparate ligand-binding sites in the human P2Y1 receptor*. Nature, 2015. **520**(7547): p. 317-321.
13. Zhang, H., H. Unal, C. Gati, Gye W. Han, W. Liu, Nadia A. Zatsepin, D. James, D. Wang, G. Nelson, U. Weierstall, Michael R. Sawaya, Q. Xu, M. Messerschmidt, Garth J. Williams, S. Boutet, Oleksandr M. Yefanov, Thomas A. White, C. Wang, A. Ishchenko, Kalyan C. Tirupula, R. Desnoyer, J. Coe, Chelsie E. Conrad, P. Fromme, Raymond C. Stevens, V. Katritch, Sadashiva S. Karnik, and V. Cherezov, *Structure of the Angiotensin Receptor Revealed by Serial Femtosecond Crystallography*. Cell, 2015. **161**(4): p. 833-844.
14. Chrencik, Jill E., Christopher B. Roth, M. Terakado, H. Kurata, R. Omi, Y. Kihara, D. Warshaviak, S. Nakade, G. Asmar-Rovira, M. Mileni, H. Mizuno, Mark T. Griffith, C. Rodgers, Gye W. Han, J. Velasquez, J. Chun, Raymond C. Stevens, and Michael A. Hanson, *Crystal Structure of Antagonist Bound Human Lysophosphatidic Acid Receptor 1*. Cell, 2015. **161**(7): p. 1633-1643.
15. Zhang, H., H. Unal, R. Desnoyer, G.W. Han, N. Patel, V. Katritch, S.S. Karnik, V. Cherezov, and R.C. Stevens, *Structural Basis for Ligand Recognition and Functional Selectivity at Angiotensin Receptor*. Journal of Biological Chemistry, 2015. **290**(49): p. 29127-29139.
16. Christopher, J.A., S.J. Aves, K.A. Bennett, A.S. Doré, J.C. Errey, A. Jazayeri, F.H. Marshall, K. Okrasa, M.J. Serrano-Vega, B.G. Tehan, G.R. Wiggin, and M. Congreve, *Fragment and Structure-Based Drug Discovery for a Class C GPCR: Discovery of the mGlu5 Negative Allosteric Modulator HTL14242 (3-Chloro-5-[6-(5-fluoropyridin-2-yl)pyrimidin-4-yl]benzonitrile)*. Journal of Medicinal Chemistry, 2015. **58**(16): p. 6653-6664.
17. Huang, C.Y., V. Olieric, P. Ma, N. Howe, L. Vogeley, X. Liu, R. Warshamanage, T. Weinert, E. Panepucci, B. Kobilka, K. Diederichs, M. Wang, and M. Caffrey, *In meso in situ serial X-ray crystallography of soluble and membrane proteins at cryogenic temperatures*. Acta Crystallogr D Struct Biol, 2016. **72**(Pt 1): p. 93-112.
18. Miller, Rebecca L., Aaron A. Thompson, C. Trapella, R. Guerrini, D. Malfacini, N. Patel, Gye W. Han, V. Cherezov, G. Caló, V. Katritch, and Raymond C. Stevens, *The Importance of Ligand-Receptor Conformational Pairs in Stabilization: Spotlight on the N/OFQ G Protein-Coupled Receptor*. Structure, 2015. **23**(12): p. 2291-2299.
19. Egloff, P., M. Hillenbrand, C. Klenk, A. Batyuk, P. Heine, S. Balada, K.M. Schlinkmann, D.J. Scott, M. Schütz, and A. Plückthun, *Structure of signaling-competent neurotensin receptor 1 obtained by directed evolution in Escherichia coli*. Proceedings of the National Academy of Sciences, 2014. **111**(6): p. E655-E662.
20. Wang, C., H. Wu, T. Evron, E. Vardy, G.W. Han, X.-P. Huang, S.J. Hufeisen, T.J. Mangano, D.J. Urban, V. Katritch, V. Cherezov, M.G. Caron, B.L. Roth, and R.C. Stevens, *Structural basis for Smoothened receptor modulation and chemoresistance to anticancer drugs*. Nat Commun, 2014. **5**.
21. Zhang, K., J. Zhang, Z.-G. Gao, D. Zhang, L. Zhu, G.W. Han, S.M. Moss, S. Paoletta, E. Kiselev, W. Lu, G. Fenalti, W. Zhang, C.E. Muller, H. Yang, H. Jiang, V. Cherezov, V. Katritch, K.A. Jacobson, R.C. Stevens, B. Wu, and Q. Zhao, *Structure of the human P2Y12 receptor in complex with an antithrombotic drug*. Nature, 2014. **509**(7498): p. 115-118.
22. Dore, A.S., K. Okrasa, J.C. Patel, M. Serrano-Vega, K. Bennett, R.M. Cooke, J.C. Errey, A. Jazayeri, S. Khan, B. Tehan, M. Weir, G.R. Wiggin, and F.H. Marshall, *Structure of class C GPCR metabotropic glutamate receptor 5 transmembrane domain*. Nature, 2014. **511**(7511): p. 557-562.

23. Wu, H., C. Wang, K.J. Gregory, G.W. Han, H.P. Cho, Y. Xia, C.M. Niswender, V. Katritch, J. Meiler, V. Cherezov, P.J. Conn, and R.C. Stevens, *Structure of a Class C GPCR Metabotropic Glutamate Receptor 1 Bound to an Allosteric Modulator*. Science, 2014. **344**(6179): p. 58-64.
24. Zhang, J., K. Zhang, Z.-G. Gao, S. Paoletta, D. Zhang, G.W. Han, T. Li, L. Ma, W. Zhang, C.E. Muller, H. Yang, H. Jiang, V. Cherezov, V. Katritch, K.A. Jacobson, R.C. Stevens, B. Wu, and Q. Zhao, *Agonist-bound structure of the human P2Y12 receptor*. Nature, 2014. **509**(7498): p. 119-122.
25. Miller, P.S. and A.R. Aricescu, *Crystal structure of a human GABAA receptor*. Nature, 2014. **512**(7514): p. 270-275.
26. Hassaine, G., C. Deluz, L. Grasso, R. Wyss, M.B. Tol, R. Hovius, A. Graff, H. Stahlberg, T. Tomizaki, A. Desmyter, C. Moreau, X.-D. Li, F. Poitevin, H. Vogel, and H. Nury, *X-ray structure of the mouse serotonin 5-HT3 receptor*. Nature, 2014. **512**(7514): p. 276-281.
27. Du, J., W. Lu, S. Wu, Y. Cheng, and E. Gouaux, *Glycine receptor mechanism elucidated by electron cryo-microscopy*. Nature, 2015. **526**(7572): p. 224-229.
28. Huang, X., H. Chen, K. Michelsen, S. Schneider, and P.L. Shaffer, *Crystal structure of human glycine receptor-[agr]3 bound to antagonist strychnine*. Nature, 2015. **526**(7572): p. 277-280.
29. Dürr, Katharina L., L. Chen, Richard A. Stein, R. De Zorzi, I.M. Folea, T. Walz, Hassane S. McHaourab, and E. Gouaux, *Structure and Dynamics of AMPA Receptor GluA2 in Resting, Pre-Open, and Desensitized States*. Cell, 2014. **158**(4): p. 778-792.
30. Meyerson, J.R., J. Kumar, S. Chittori, P. Rao, J. Pierson, A. Bartesaghi, M.L. Mayer, and S. Subramaniam, *Structural mechanism of glutamate receptor activation and desensitization*. Nature, 2014. **514**(7522): p. 328-334.
31. Yelshanskaya, M.V., M. Li, and A.I. Sobolevsky, *Structure of an agonist-bound ionotropic glutamate receptor*. Science, 2014. **345**(6200): p. 1070-1074.
32. Chen, L., K.L. Dürr, and E. Gouaux, *X-ray structures of AMPA receptor–cone snail toxin complexes illuminate activation mechanism*. Science, 2014. **345**(6200): p. 1021-1026.
33. Lee, C.-H., W. Lu, J.C. Michel, A. Goehring, J. Du, X. Song, and E. Gouaux, *NMDA receptor structures reveal subunit arrangement and pore architecture*. Nature, 2014. **511**(7508): p. 191-197.
34. Karakas, E. and H. Furukawa, *Crystal structure of a heterotetrameric NMDA receptor ion channel*. Science, 2014. **344**(6187): p. 992-997.
35. Fan, G., M.L. Baker, Z. Wang, M.R. Baker, P.A. Sinyagovskiy, W. Chiu, S.J. Ludtke, and I.I. Serysheva, *Gating machinery of InsP3R channels revealed by electron cryomicroscopy*. Nature, 2015. **527**(7578): p. 336-341.
36. Zalk, R., O.B. Clarke, A. des Georges, R.A. Grassucci, S. Reiken, F. Mancia, W.A. Hendrickson, J. Frank, and A.R. Marks, *Structure of a mammalian ryanodine receptor*. Nature, 2015. **517**(7532): p. 44-49.
37. Yan, Z., X.-c. Bai, C. Yan, J. Wu, Z. Li, T. Xie, W. Peng, C.-c. Yin, X. Li, S.H.W. Scheres, Y. Shi, and N. Yan, *Structure of the rabbit ryanodine receptor RyR1 at near-atomic resolution*. Nature, 2015. **517**(7532): p. 50-55.
38. Kane Dickson, V., L. Pedi, and S.B. Long, *Structure and insights into the function of a Ca2+-activated Cl- channel*. Nature, 2014. **516**(7530): p. 213-218.
39. Wu, J., Z. Yan, Z. Li, C. Yan, S. Lu, M. Dong, and N. Yan, *Structure of the voltage-gated calcium channel Cav1.1 complex*. Science, 2015. **350**(6267).
40. Liao, M., E. Cao, D. Julius, and Y. Cheng, *Structure of the TRPV1 ion channel determined by electron cryo-microscopy*. Nature, 2013. **504**(7478): p. 107-112.

41. Paulsen, C.E., J.-P. Armache, Y. Gao, Y. Cheng, and D. Julius, *Structure of the TRPA1 ion channel suggests regulatory mechanisms*. Nature, 2015. **520**(7548): p. 511-517.
42. Schredelseker, J., A. Paz, C.J. López, C. Altenbach, C.S. Leung, M.K. Drexler, J.-N. Chen, W.L. Hubbell, and J. Abramson, *High Resolution Structure and Double Electron-Electron Resonance of the Zebrafish Voltage-dependent Anion Channel 2 Reveal an Oligomeric Population*. Journal of Biological Chemistry, 2014. **289**(18): p. 12566-12577.
43. Choudhary, O.P., A. Paz, J.L. Adelman, J.-P. Colletier, J. Abramson, and M. Grabe, *Structure-guided simulations illuminate the mechanism of ATP transport through VDAC1*. Nat Struct Mol Biol, 2014. **21**(7): p. 626-632.
44. Takeshita, K., S. Sakata, E. Yamashita, Y. Fujiwara, A. Kawanabe, T. Kurokawa, Y. Okochi, M. Matsuda, H. Narita, Y. Okamura, and A. Nakagawa, *X-ray crystal structure of voltage-gated proton channel*. Nat Struct Mol Biol, 2014. **21**(4): p. 352-357.
45. Ahuja, S., S. Mukund, L. Deng, K. Khakh, E. Chang, H. Ho, S. Shriver, C. Young, S. Lin, J.P. Johnson, P. Wu, J. Li, M. Coons, C. Tam, B. Brillantes, H. Sampang, K. Mortara, K.K. Bowman, K.R. Clark, A. Estevez, Z. Xie, H. Verschoof, M. Grimwood, C. Dehnhardt, J.-C. Andrez, T. Focken, D.P. Sutherlin, B.S. Safina, M.A. Starovasnik, D.F. Ortwine, Y. Franke, C.J. Cohen, D.H. Hackos, C.M. Koth, and J. Payandeh, *Structural basis of Nav1.7 inhibition by an isoform-selective small-molecule antagonist*. Science, 2015. **350**(6267).
46. Baconguis, I., Christopher J. Bohlen, A. Goehring, D. Julius, and E. Gouaux, *X-Ray Structure of Acid-Sensing Ion Channel 1–Snake Toxin Complex Reveals Open State of a Na+-Selective Channel*. Cell, 2014. **156**(4): p. 717-729.
47. Gonzales, E.B., T. Kawate, and E. Gouaux, *Pore architecture and ion sites in acid-sensing ion channels and P2X receptors*. Nature, 2009. **460**(7255): p. 599-604.
48. Dong, Y.Y., A.C.W. Pike, A. Mackenzie, C. McClenaghan, P. Aryal, L. Dong, A. Quigley, M. Grieben, S. Goubin, S. Mukhopadhyay, G.F. Ruda, M.V. Clausen, L. Cao, P.E. Brennan, N.A. Burgess-Brown, M.S.P. Sansom, S.J. Tucker, and E.P. Carpenter, *K2P channel gating mechanisms revealed by structures of TREK-2 and a complex with Prozac*. Science, 2015. **347**(6227): p. 1256-1259.
49. Brohawn, S.G., E.B. Campbell, and R. MacKinnon, *Physical mechanism for gating and mechanosensitivity of the human TRAAK K+ channel*. Nature, 2014. **516**(7529): p. 126-130.
50. Hite, R.K., P. Yuan, Z. Li, Y. Hsuing, T. Walz, and R. MacKinnon, *Cryo-electron microscopy structure of the Slo2.2 Na+-activated K+ channel*. Nature, 2015. **527**(7577): p. 198-203.
51. Ge, J., W. Li, Q. Zhao, N. Li, M. Chen, P. Zhi, R. Li, N. Gao, B. Xiao, and M. Yang, *Architecture of the mammalian mechanosensitive Piezo1 channel*. Nature, 2015. **527**(7576): p. 64-69.
52. Suzuki, H., T. Nishizawa, K. Tani, Y. Yamazaki, A. Tamura, R. Ishitani, N. Dohmae, S. Tsukita, O. Nureki, and Y. Fujiyoshi, *Crystal Structure of a Claudin Provides Insight into the Architecture of Tight Junctions*. Science, 2014. **344**(6181): p. 304-307.
53. Saitoh, Y., H. Suzuki, K. Tani, K. Nishikawa, K. Irie, Y. Ogura, A. Tamura, S. Tsukita, and Y. Fujiyoshi, *Structural insight into tight junction disassembly by Clostridium perfringens enterotoxin*. Science, 2015. **347**(6223): p. 775-778.
54. Penmatsa, A., K.H. Wang, and E. Gouaux, *X-ray structures of Drosophila dopamine transporter in complex with nisoxetine and reboxetine*. Nat Struct Mol Biol, 2015. **22**(6): p. 506-508.

55. Wang, K.H., A. Penmatsa, and E. Gouaux, *Neurotransmitter and psychostimulant recognition by the dopamine transporter*. Nature, 2015. **521**(7552): p. 322-327.
56. Srinivasan, V., A.J. Pierik, and R. Lill, *Crystal Structures of Nucleotide-Free and Glutathione-Bound Mitochondrial ABC Transporter Atm1*. Science, 2014. **343**(6175): p. 1137-1140.
57. Kodan, A., T. Yamaguchi, T. Nakatsu, K. Sakiyama, C.J. Hipolito, A. Fujioka, R. Hirokane, K. Ikeguchi, B. Watanabe, J. Hiratake, Y. Kimura, H. Suga, K. Ueda, and H. Kato, *Structural basis for gating mechanisms of a eukaryotic P-glycoprotein homolog*. Proceedings of the National Academy of Sciences, 2014. **111**(11): p. 4049-4054.
58. Szewczyk, P., H. Tao, A.P. McGrath, M. Villaluz, S.D. Rees, S.C. Lee, R. Doshi, I.L. Urbatsch, Q. Zhang, and G. Chang, *Snapshots of ligand entry, malleable binding and induced helical movement in P-glycoprotein*. Acta Crystallogr D Biol Crystallogr, 2015. **71**(Pt 3): p. 732-41.
59. Yonekura, K., K. Kato, M. Ogasawara, M. Tomita, and C. Toyoshima, *Electron crystallography of ultrathin 3D protein crystals: Atomic model with charges*. Proceedings of the National Academy of Sciences, 2015. **112**(11): p. 3368-3373.
60. Drachmann, N.D., C. Olesen, J.V. Møller, Z. Guo, P. Nissen, and M. Bublitz, *Comparing crystal structures of Ca2+-ATPase in the presence of different lipids*. FEBS Journal, 2014. **281**: p. 4249-4262.
61. Akin, B.L., T.D. Hurley, Z. Chen, and L.R. Jones, *The Structural Basis for Phospholamban Inhibition of the Calcium Pump in Sarcoplasmic Reticulum*. Journal of Biological Chemistry, 2013. **288**(42): p. 30181-30191.
62. Takahashi, M., Y. Kondou, and C. Toyoshima, *Interdomain communication in calcium pump as revealed in the crystal structures with transmembrane inhibitors*. Proceedings of the National Academy of Sciences, 2007. **104**(14): p. 5800-5805.
63. Morita, M., H. Ogawa, O. Ohno, T. Yamori, K. Suenaga, and C. Toyoshima, *Biselyngbyasides, cytotoxic marine macrolides, are novel and potent inhibitors of the Ca2+ pumps with a unique mode of binding*. FEBS Letters, 2015. **589**: p. 1406-1411.
64. Bublitz, M., K. Nass, N.D. Drachmann, A.J. Markvardsen, M.J. Gutmann, T.R.M. Barends, D. Mattle, R.L. Shoeman, R.B. Doak, S. Boutet, M. Messerschmidt, M.M. Seibert, G.J. Williams, L. Foucar, L. Reinhard, O. Sitsel, J.L. Gregersen, J.D. Clausen, T. Boesen, K. Gotfryd, K.-T. Wang, C. Olesen, J.V. Møller, P. Nissen, and I. Schlichting, *Structural studies of P-type ATPase–ligand complexes using an X-ray free-electron laser*. IUCrJ, 2015. **2**(Pt 4): p. 409-420.
65. Laursen, M., J.L. Gregersen, L. Yatime, P. Nissen, and N.U. Fedosova, *Structures and characterization of digoxin- and bufalin-bound Na+,K+-ATPase compared with the ouabain-bound complex*. Proceedings of the National Academy of Sciences, 2015. **112**(6): p. 1755-1760.
66. Ogawa, H., F. Cornelius, A. Hirata, and C. Toyoshima, *Sequential substitution of K+ bound to Na+,K+-ATPase visualized by X-ray crystallography*. Nat Commun, 2015. **6**.
67. Balakrishna, Asha M., H. Seelert, S.-H. Marx, Norbert A. Dencher, and G. Grüber, *Crystallographic structure of the turbine C-ring from spinach chloroplast F-ATP synthase*. Bioscience Reports, 2014. **34**(2): p. e00102.
68. Symersky, J., D. Osowski, D.E. Walters, and D.M. Mueller, *Oligomycin frames a common drug-binding site in the ATP synthase*. Proceedings of the National Academy of Sciences, 2012. **109**(35): p. 13961-13965.
69. Zhao, J., S. Benlekbir, and J.L. Rubinstein, *Electron cryomicroscopy observation of rotational states in a eukaryotic V-ATPase*. Nature, 2015. **521**(7551): p. 241-245.

70. Deng, D., C. Xu, P. Sun, J. Wu, C. Yan, M. Hu, and N. Yan, *Crystal structure of the human glucose transporter GLUT1*. Nature, 2014. **510**(7503): p. 121-125.
71. Deng, D., P. Sun, C. Yan, M. Ke, X. Jiang, L. Xiong, W. Ren, K. Hirata, M. Yamamoto, S. Fan, and N. Yan, *Molecular basis of ligand recognition and transport by glucose transporters*. Nature, 2015. **526**(7573): p. 391-396.
72. Nomura, N., G. Verdon, H.J. Kang, T. Shimamura, Y. Nomura, Y. Sonoda, S.A. Hussien, A.A. Qureshi, M. Coincon, Y. Sato, H. Abe, Y. Nakada-Nakura, T. Hino, T. Arakawa, O. Kusano-Arai, H. Iwanari, T. Murata, T. Kobayashi, T. Hamakubo, M. Kasahara, S. Iwata, and D. Drew, *Structure and mechanism of the mammalian fructose transporter GLUT5*. Nature, 2015. **526**(7573): p. 397-401.
73. Tao, Y., L.S. Cheung, S. Li, J.-S. Eom, L.-Q. Chen, Y. Xu, K. Perry, W.B. Frommer, and L. Feng, *Structure of a eukaryotic SWEET transporter in a homotrimeric complex*. Nature, 2015. **527**(7577): p. 259-263.
74. Sun, J., J.R. Bankston, J. Payandeh, T.R. Hinds, W.N. Zagotta, and N. Zheng, *Crystal structure of the plant dual-affinity nitrate transporter NRT1.1*. Nature, 2014. **507**(7490): p. 73-77.
75. Parker, J.L. and S. Newstead, *Molecular basis of nitrate uptake by the plant nitrate transporter NRT1.1*. Nature, 2014. **507**(7490): p. 68-72.
76. Brunner, J.D., N.K. Lim, S. Schenck, A. Duerst, and R. Dutzler, *X-ray structure of a calcium-activated TMEM16 lipid scramblase*. Nature, 2014. **516**(7530): p. 207-212.
77. Frick, A., U.K. Eriksson, F. de Mattia, F. Öberg, K. Hedfalk, R. Neutze, W.J. de Grip, P.M.T. Deen, and S. Törnroth-Horsefield, *X-ray structure of human aquaporin 2 and its implications for nephrogenic diabetes insipidus and trafficking*. Proceedings of the National Academy of Sciences, 2014. **111**(17): p. 6305-6310.
78. Kitchen, P., F. Öberg, J. Sjöhamn, K. Hedfalk, R.M. Bill, A.C. Conner, M.T. Conner, and S. Törnroth-Horsefield, *Plasma Membrane Abundance of Human Aquaporin 5 Is Dynamically Regulated by Multiple Pathways*. PLoS ONE, 2015. **10**(11): p. e0143027.
79. Bellomio, A., K. Morante, A. Barlič, I. Gutiérrez-Aguirre, A.R. Viguera, and J.M. González-Mañas, *Purification, cloning and characterization of fragaceatoxin C, a novel actinoporin from the sea anemone Actinia fragacea*. Toxicon, 2009. **54**(6): p. 869-880.
80. Jaremko, Ł., M. Jaremko, K. Giller, S. Becker, and M. Zweckstetter, *Structure of the Mitochondrial Translocator Protein in Complex with a Diagnostic Ligand*. Science, 2014. **343**(6177): p. 1363-1366.
81. Jaremko, M., Ł. Jaremko, K. Giller, S. Becker, and M. Zweckstetter, *Structural Integrity of the A147T Polymorph of Mammalian TSPO*. ChemBioChem, 2015. **16**(10): p. 1483-1489.
82. Vinothkumar, K.R., J. Zhu, and J. Hirst, *Architecture of mammalian respiratory complex I*. Nature, 2014. **515**(7525): p. 80-4.
83. Capper, M.J., P.M. O'Neill, N. Fisher, R.W. Strange, D. Moss, S.A. Ward, N.G. Berry, A.S. Lawrenson, S.S. Hasnain, G.A. Biagini, and S.V. Antonyuk, *Antimalarial 4(1H)-pyridones bind to the Qi site of cytochrome bc1*. Proceedings of the National Academy of Sciences, 2015. **112**(3): p. 755-760.
84. Birth, D., W.-C. Kao, and C. Hunte, *Structural analysis of atovaquone-inhibited cytochrome bc1 complex reveals the molecular basis of antimalarial drug action*. Nat Commun, 2014. **5**.
85. Yano, N., K. Muramoto, M. Mochizuki, K. Shinzawa-Itoh, S. Yoshikawa, and T. Tsukihara, *X-ray structure of cyanide-bound bovine heart cytochrome c oxidase in the fully oxidized state at 2.0 A resolution*. Acta Crystallographica Section F, 2015. **71**: p. 726-730.

86. Lu, P., D. Ma, C. Yan, X. Gong, M. Du, and Y. Shi, *Structure and mechanism of a eukaryotic transmembrane ascorbate-dependent oxidoreductase*. Proceedings of the National Academy of Sciences, 2014. **111**(5): p. 1813-1818.
87. Inaoka, D.K., T. Shiba, D. Sato, E.O. Balogun, T. Sasaki, M. Nagahama, M. Oda, S. Matsuoka, J. Ohmori, T. Honma, M. Inoue, K. Kita, and S. Harada, *Structural Insights into the Molecular Design of Flutolanil Derivatives Targeted for Fumarate Respiration of Parasite Mitochondria*. International Journal of Molecular Sciences, 2015. **16**(7): p. 15287-15308.
88. Fan, M., M. Li, Z. Liu, P. Cao, X. Pan, H. Zhang, X. Zhao, J. Zhang, and W. Chang, *Crystal structures of the PsbS protein essential for photoprotection in plants*. Nat Struct Mol Biol, 2015. **22**(9): p. 729-735.
89. Wan, T., M. Li, X. Zhao, J. Zhang, Z. Liu, and W. Chang, *Crystal Structure of a Multilayer Packed Major Light-Harvesting Complex: Implications for Grana Stacking in Higher Plants*. Molecular Plant, 2014. **7**(5): p. 916-919.
90. Qin, X., M. Suga, T. Kuang, and J.-R. Shen, *Structural basis for energy transfer pathways in the plant PSI-LHCI supercomplex*. Science, 2015. **348**(6238): p. 989-995.
91. Tanabe, H., Y. Fujii, M. Okada-Iwabu, M. Iwabu, Y. Nakamura, T. Hosaka, K. Motoyama, M. Ikeda, M. Wakiyama, T. Terada, N. Ohsawa, M. Hato, S. Ogasawara, T. Hino, T. Murata, S. Iwata, K. Hirata, Y. Kawano, M. Yamamoto, T. Kimura-Someya, M. Shirouzu, T. Yamauchi, T. Kadowaki, and S. Yokoyama, *Crystal structures of the human adiponectin receptors*. Nature, 2015. **520**(7547): p. 312-316.
92. Monk, B.C., T.M. Tomasiak, M.V. Keniya, F.U. Huschmann, J.D.A. Tyndall, J.D. O'Connell, R.D. Cannon, J.G. McDonald, A. Rodriguez, J.S. Finer-Moore, and R.M. Stroud, *Architecture of a single membrane spanning cytochrome P450 suggests constraints that orient the catalytic domain relative to a bilayer*. Proceedings of the National Academy of Sciences, 2014. **111**(10): p. 3865-3870.
93. Bennett, B.C., M.D. Purdy, K.A. Baker, C. Acharya, W.E. McIntire, R.C. Stevens, Q. Zhang, A.L. Harris, R. Abagyan, and M. Yeager, *An electrostatic mechanism for Ca2+-mediated regulation of gap junction channels*. Nat Commun, 2016. **7**.
94. Ruprecht, J.J., A.M. Hellawell, M. Harding, P.G. Crichton, A.J. McCoy, and E.R.S. Kunji, *Structures of yeast mitochondrial ADP/ATP carriers support a domain-based alternating-access transport mechanism*. Proceedings of the National Academy of Sciences, 2014. **111**(4): p. E426-E434.
95. Bai, Y., J.G. McCoy, E.J. Levin, P. Sobrado, K.R. Rajashankar, B.G. Fox, and M. Zhou, *X-ray structure of a mammalian stearoyl-CoA desaturase*. Nature, 2015. **524**(7564): p. 252-256.
96. Wang, H., M.G. Klein, H. Zou, W. Lane, G. Snell, I. Levin, K. Li, and B.-C. Sang, *Crystal structure of human stearoyl-coenzyme A desaturase in complex with substrate*. Nat Struct Mol Biol, 2015. **22**(7): p. 581-585.
97. Niegowski, D., T. Kleinschmidt, U. Olsson, S. Ahmad, A. Rinaldo-Matthis, and J.Z. Haeggström, *Crystal Structures of Leukotriene C(4) Synthase in Complex with Product Analogs: IMPLICATIONS FOR THE ENZYME MECHANISM*. The Journal of Biological Chemistry, 2014. **289**(8): p. 5199-5207.
98. Li, D., N. Howe, A. Dukkipati, S.T.A. Shah, B.D. Bax, C. Edge, A. Bridges, P. Hardwicke, O.M.P. Singh, G. Giblin, A. Pautsch, R. Pfau, G. Schnapp, M. Wang, V. Olieric, and M. Caffrey, *Crystallizing Membrane Proteins in the Lipidic Mesophase. Experience with Human Prostaglandin E2 Synthase 1 and an Evolving Strategy*. Crystal Growth & Design, 2014. **14**(4): p. 2034-2047.
99. Arakawa, T., T. Kobayashi-Yurugi, Y. Alguel, H. Iwanari, H. Hatae, M. Iwata, Y. Abe, T. Hino, C. Ikeda-Suno, H. Kuma, D. Kang, T. Murata, T. Hamakubo, A.D. Cameron,

T. Kobayashi, N. Hamasaki, and S. Iwata, *Crystal structure of the anion exchanger domain of human erythrocyte band 3*. Science, 2015. **350**(6261): p. 680-684.
100. Sun, L., L. Zhao, G. Yang, C. Yan, R. Zhou, X. Zhou, T. Xie, Y. Zhao, S. Wu, X. Li, and Y. Shi, *Structural basis of human γ-secretase assembly*. Proceedings of the National Academy of Sciences, 2015. **112**(19): p. 6003-6008.
101. Bai, X.-c., C. Yan, G. Yang, P. Lu, D. Ma, L. Sun, R. Zhou, S.H.W. Scheres, and Y. Shi, *An atomic structure of human [ggr]-secretase*. Nature, 2015. **525**(7568): p. 212-217.
102. Trenker, R., M.E. Call, and M.J. Call, *Crystal Structure of the Glycophorin A Transmembrane Dimer in Lipidic Cubic Phase*. Journal of the American Chemical Society, 2015. **137**(50): p. 15676-15679.
103. Bragin, P.E., K.S. Mineev, O.V. Bocharova, P.E. Volynsky, E.V. Bocharov, and A.S. Arseniev, *HER2 Transmembrane Domain Dimerization Coupled with Self-Association of Membrane-Embedded Cytoplasmic Juxtamembrane Regions*. Journal of Molecular Biology, 2016. **428**(1): p. 52-61.
104. Li, Q., S. Wanderling, M. Paduch, D. Medovoy, A. Singharoy, R. McGreevy, C.A. Villalba-Galea, R.E. Hulse, B. Roux, K. Schulten, A. Kossiakoff, and E. Perozo, *Structural mechanism of voltage-dependent gating in an isolated voltage-sensing domain*. Nat Struct Mol Biol, 2014. **21**(3): p. 244-52.
105. Kato, H.E., M. Kamiya, S. Sugo, J. Ito, R. Taniguchi, A. Orito, K. Hirata, A. Inutsuka, A. Yamanaka, A.D. Maturana, R. Ishitani, Y. Sudo, S. Hayashi, and O. Nureki, *Atomistic design of microbial opsin-based blue-shifted optogenetics tools*. Nat Commun, 2015. **6**.
106. Zickermann, V., C. Wirth, H. Nasiri, K. Siegmund, H. Schwalbe, C. Hunte, and U. Brandt, *Mechanistic insight from the crystal structure of mitochondrial complex I*. Science, 2015. **347**(6217): p. 44-49.
107. Knoblich, K., S. Park, M. Lutfi, L. van 't Hag, Charlotte E. Conn, Shane A. Seabrook, J. Newman, Peter E. Czabotar, W. Im, Matthew E. Call, and Melissa J. Call, *Transmembrane Complexes of DAP12 Crystallized in Lipid Membranes Provide Insights into Control of Oligomerization in Immunoreceptor Assembly*. Cell Reports, 2015. **11**(8): p. 1184-1192.